Advanced Drug Delivery Reviews 61 (2009) 988–1006

Contents lists available at ScienceDirect

Advanced Drug Delivery Reviews

journal homepage: www.elsevier.com/locate/addr

Electrospun silk biomaterial scaffolds for regenerative medicine ☆

Xiaohui Zhang [a], Michaela R. Reagan [b], David L. Kaplan [a,b,*]

[a] Department of Chemical and Biological Engineering, Tufts University, 4 Colby Street, Medford, MA 02155, USA
[b] Department of Biomedical Engineering, Tufts University, 4 Colby Street, Medford, MA 02155, USA

ARTICLE INFO

Article history:
Received 23 January 2009
Accepted 16 July 2009
Available online 28 July 2009

Keywords:
Silk
Biomaterials
Electrospinning
Nanofiber
Tissue engineering
Matrices
Scaffolds

ABSTRACT

Electrospinning is a versatile technique that enables the development of nanofiber-based biomaterial scaffolds. Scaffolds can be generated that are useful for tissue engineering and regenerative medicine since they mimic the nanoscale properties of certain fibrous components of the native extracellular matrix in tissues. Silk is a natural protein with excellent biocompatibility, remarkable mechanical properties as well as tailorable degradability. Integrating these protein polymer advantages with electrospinning results in scaffolds with combined biochemical, topographical and mechanical cues with versatility for a range of biomaterial, cell and tissue studies and applications. This review covers research related to electrospinning of silk, including process parameters, post treatment of the spun fibers, functionalization of nanofibers, and the potential applications for these material systems in regenerative medicine. Research challenges and future trends are also discussed.

Contents

1. Introduction

Continuous progress in medical science and surgical technologies has allowed tissue or whole-organ transplantation to become potential options to restore native functions for many damaged parts of the human body. Unfortunately, the increasing demand for transplants far exceeds the available supply of usable donor tissues. Along with other issues such as immunological problems and possible

☆ This review is part of the *Advanced Drug Delivery Reviews* theme issue on "Nanofibers in Regenerative Medicine & Drug Delivery".

* Corresponding author. Department of Biomedical Engineering, Tufts University, 4 Colby Street, Medford, MA 02155, USA. Tel.: +617 627 3251; fax: +617 627 3231.
E-mail address: david.kaplan@tufts.edu (D.L. Kaplan).

0169-409X/$ – see front matter © 2009 Elsevier B.V. All rights reserved.
doi:10.1016/j.addr.2009.07.005

contamination of donor tissue, transplantation technology has encountered severe limitations. Therefore, new technology is needed to reduce this gap in clinical need versus available healthy tissue and organ supplies. Tissue engineering/regenerative medicine has emerged as a new and versatile approach for the repair/regeneration of damage tissue, with the potential to circumvent the limitations of traditional therapies [1–4].

Tissue engineering represents an interdisciplinary field employing principles and methods of engineering and life sciences. The field is aimed at a fundamental understanding of structure–function relationships in normal and pathological mammalian tissue, as a route to develop novel biological substitutes, which are capable of regenerating tissue functions that would otherwise fail to regenerate spontaneously [4,5]. Tissue engineering takes many forms, but essentially involves the process of harvesting relevant cells from a patient or donor, expanding or manipulating the cells *in vitro*, seeding these cells into a three-dimensional (3-D) scaffold and inducing them to proliferate, differentiate and eventually develop into a desired tissue for implantation. In this regard, at least three key factors should be considered for successful tissue regeneration: (i) the cells that will form the tissue, (ii) the scaffold that provides structural and anchoring support to the cells, and (iii) cell–matrix (scaffold) interactions that direct tissue growth [6]. The scaffold serves as a mimic for the native extracellular matrix (ECM) and plays a pivotal role in tissue regeneration by providing temporary support for the cells during the formation of a more natural ECM by the cells. The scaffold also plays a critical role in providing the appropriate chemical, morphological and structural cues to direct the cells towards a targeted functional outcome. Therefore, scaffold design has become one of the central themes in regenerative medicine and a great deal of effort is spent on designing suitable scaffold systems to optimize cell and tissue outcomes.

A great deal of effort has been put into the design of artificial matrices (scaffolds), and the concept has evolved from inert biomaterials serving as structural support for cells, to more complex, dynamic biomaterial environments to direct cells towards desired outcomes in terms of tissue development. The ultimate goal is to enable the host body, particularly the cellular components, to recognize the introduced artificial matrix, and in turn, to regenerate "neo-native" functional tissue. Therefore, a useful approach to design tissue-engineered scaffolds is to mimic the natural ECM [7]. However, there is no guidance as to which characteristics define scaffolds for optimized cell and tissue responses, coupled with the fact that the native ECM in the body is complex, dynamic and tissue specific. Therefore, the characteristics of a scaffold vary according to tissue type.

However, there are several general characteristics considered essential for scaffold design that can serve as a reasonable starting point [8,9]. The first requirement is that the material should be biocompatible, able to support appropriate cellular activity to optimize tissue regeneration without eliciting undesirable local or systemic responses, such as rejection, inflammation or immune activation, in the host. Secondly, the scaffold should have a porous architecture with high surface area to allow for maximum cell loading and cell–matrix interactions, as well as to improve transport into and out of the matrix for nutrients and oxygen. Moreover, this structure is desirable for locally sequestering and delivering bioactive molecules, and providing space for tissue in-growth. In addition, most tissue engineering applications and tissue regeneration approaches require scaffolds that are fully biodegradable or absorbable. It is useful if the degradation rate of the scaffold matches the rate of tissue regeneration to optimize the transfer of functions from the artificial matrices to native ECM on a time-dependent basis during tissue regeneration. Faster rates of degradation of the scaffold may lead to a loss of tissue integrity and function, while a degradation rate that is too slow can result in barriers to transport or mechanical mismatches such as stress shielding, resulting in long-term failure of the system. Scaffolds should also be mechanically matched to the target tissue, sterilizable without compromising structural or other related properties and for clinical success the production of scaffold must be reproducible, economical and scalable. Collectively, these general rules for scaffold design are focused more at the macroscopic level. In order to realize the active role of artificial scaffolds in regulating the behavior of cells, the interface between the biomaterial and the cells must be examined.

In native tissue, the extracellular matrix is mainly composed of two classes of macromolecules: (i) polysaccharide chains of the class called glycosaminoglycans (GAGs), which are usually found covalently linked to protein in the form of proteoglycans, and (ii) fibrous proteins, including collagens, elastin, fibronectin, and laminin, which have both structural and adhesive functions. The proteoglycan molecules form highly hydrated gels, in which the assembled fibrous proteins are embedded and interact with cells through mechanical as well as chemical signals [10,11]. For example, fibroblasts can reorganize the collagen they have secreted and compact it into nanoscale fibrils at various sizes and arrangements, which changes the architecture of the tissue. On the other hand, extracellular signals, such as organization of the matrix protein, can regulate the organization of the cytoskeleton of cells, thus influencing cell spreading. The diameter of these structural ECM proteins (50 to 500 nm) is about 1–2 orders of magnitude smaller than the cells, which is critical for cells in order to be able to recognize the architecture of the ECM and define its three dimensional (3D) orientation [12,13]. This feature may be important for artificial scaffold designs that use nanoscale structures.

Nanotechnology, specifically nanofibers, for a more suitable format of artificial matrices for tissue engineering applications, has become an important direction to consider in the field based on the above structural features of the native ECM. Conventional polymer fiber processing techniques usually produce fibers tens of microns in diameter, which are several orders of magnitude larger than those in the native ECM. With progress in nanotechnology, nanofibers to more adequately simulate ECM geometry can be produced by self-assembly, phase separation and electrospinning [14–17]. Self-assembly generally generates nanofibers 5–8 nm in diameter, at the small end of the natural ECM scale. However, the complexity and low productivity of this technique limits its application as tissue engineered scaffolds [15]. Further, these matrices tend to be relatively soft or nonstructured in comparison to the other processing options. Unlike self-assembly, phase separation is a simple technique that does not require specialized equipment, and generates fibers with diameters from 50–500 nm, similar to natural collagen fibers in ECM. However, this method is effective with only a selected number of polymers and not feasible for scale-up [14]. Electrospinning is a unique nanofiber approach that has attracted attention as it is simple, inexpensive and can be scaled-up. Moreover, a diverse set of polymers can be used to produce fibers from a few micrometers down to the tens of nanometers in diameter by adjusting process parameters [18]. Thus scaffolds with desired geometries and properties can be manipulated by selecting suitable material/composite components along with processing parameters.

Silk-based biomaterials have demonstrated excellent biocompatibility in different material formats for various tissue regenerations [19–21]. Moreover, the unique structural assembly of this protein endows it with remarkable mechanical properties when compared with other commonly used biopolymer-based biomaterials [22]. The degradation rate can be tailored from months to years after implanting *in vivo*, based on processing procedures employed during material formation [23]. Finally, the thermal stability of silk biomaterials allow processing over a wide range of temperatures up to about 250 °C, as evidenced by the ability to autoclave silk material systems without loss of functional integrity [24–26].

In this review, a brief overview is provided for the potential for using silk proteins with electrospinning for tissue regeneration. The parameters relevant to the electrospinning process of silk proteins are

described, along with various tissue-specific regeneration applications. Research challenges and future trends are also addressed.

2. Electrospinning silk proteins

2.1. Evolution and principle of electrospinning

The process of 'electrospinning', previously known as 'electrostatic spinning', was first investigated by Zeleny in 1914, and was found to be a feasible technique for spinning small-diameter polymer fibers [27]. However, technical difficulties related to fiber formation impeded development until 1934, when Formhals was issued the first US patent for the process of spinning synthetic fibers and an apparatus used in this procedure [28]. In this patent, cellulose acetate dissolved in acetone/alcohol solution was spun into fibers which were gathered on a movable collector. Following the initial patent, the process of developing nanofibers from a wide range of polymers using the electrospinning technique has ensued [29–34].

After this preliminary success, the focus of electrospinning turned to advancing the understanding of the mechanisms of the fiber formation. In 1969, Taylor published his work regarding the jet forming process [35], in which for the first time he described the phenomena of Taylor cone, which develops from the pendant droplet when the electrostatic forces are balanced by surface tension. In this study, Taylor also observed the emission of a fiber jet from the apex of the cone, which explained the generation of fibers with significantly smaller diameters compared to the spinneret. Shortly after the discovery of the Taylor cone, interest in the field shifted to a more thorough understanding of the relationship between electrospinning processing/solution parameters and the structural characteristics of the resulting fibers. In 1971, Baumgarten studied the effects of solution and processing parameters on the structure of electrospun fibers using a polyacrylonitrile/dimethylformamide (PAN/DMF) solution. He discovered a positive relationship between fiber diameter and solution viscosity [33]. Concurrently, other researchers began to examine the potential of electrospun fibrous matrices for other applications. In 1978, Annis and Bornat evaluated the feasibility of electrospun polyurethane mats as vascular prostheses [36]. By 1985, Fisher and Annis had assessed the long-term *in vivo* performance of electrospun arterial prostheses. However, little work has been done to follow up on these earlier efforts [37].

Electrospinning regained attention in the 1990s partly due to interest in nanotechnology, as the process allowed easy fabrication of fibers with nanoscale diameters from various polymers [38]. Revival of the electrospinning technique was marked by an increase in publications on the subject after 1998 [38]. To date, more than 50 different polymers have been successfully electrospun into ultrafine fibers. In the early 1990s, non-degradable polymers, such as polyamides [39], polyurethanes [40], polyesters [41] and a wide range of vinyl polymers [42] were often employed for applications such as which are mostly used for novel filtration devices [43], efficient catalysts, nanoelectronic devices or protective military clothing [42]. Many synthetic biodegradable and natural polymers, as listed in Table 1, have been tested for nanofiber fabrication as electrospinning entered the field of biomedical applications. These polymers have been heavily tested, especially for use in tissue engineering and drug delivery applications [42].

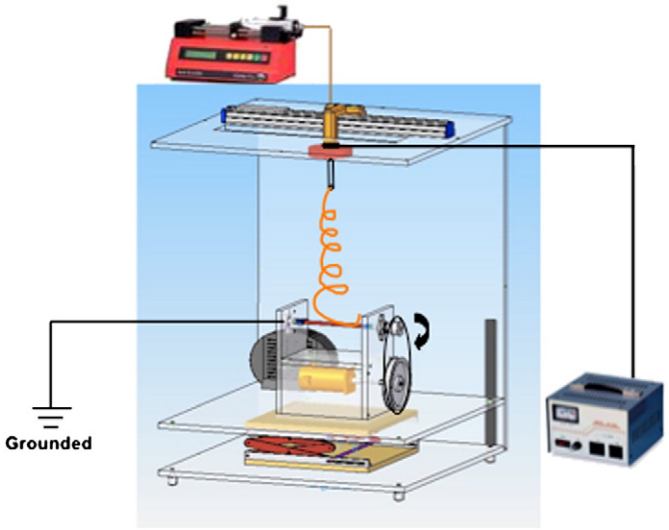

Fig. 1. Schematic diagram of electrospinning setup.

It has been almost 100 years since the discovery of the electrospinning process for generation of polymer fibers. However, little of the process has changed since Formhals described it in his first patent. A typical electrospinning setup consists of three components: a high voltage supplier, a capillary needle or pipette, and a grounded collector (Fig. 1). During electrospinning, an electric potential is applied to a pendent droplet of polymer solution suspended from a needle or pipette, usually delivered with a syringe pump or by gravitational force [44,45]. Repulsive forces produced by like charges in the solution as well as the attractive forces between the liquid and the collector work together to exert tensile forces on the solution. Surface tension and viscoelastic forces of the polymer solution retain the hemispherical shape of the suspended droplet, while the electric force pulls the droplet away from the capillary [46]. As the applied voltage is increased beyond a critical value, where the electrostatic forces balance out the surface tension of the droplet at the tip of the capillary, the development of the Taylor cone occurs. As a result, a fiber jet ejects

Table 1
Electrospun materials used in tissue engineering.

Polymer		Solvent	Fiber diameter (nm)	Target tissues/cell types	References
Synthetic	Poly(lactic acid) (PLA)	DMF/DCM	300–3500	Nerve	[142]
	Poly(glycolic acid) (PGA)	DMF/THF	500–800	hMSC	[143]
	Poly(lactide-co-glycolide) (PLGA)	HFP	720	Blood vessel	[144]
	Poly(ε-caprolactone) (PCL)	Chloroform/DMF	200–1000	Blood vessel	[145]
		Chloroform/methanol	559	Nerve	[146]
	Poly(L-lactide-co-ε-caprolactone) (PLCL)	HFP	792–820	Blood vessel	[147]
		Acetone	200–800	Blood vessel	[110]
Natural	Collagen	HFP	10–730	Blood vessel	[148]
	Gelatin	TFE	290–9100	–	[149]
	Hyaluronic acid	HCL	49–74	–	[150]
	Silk	Water	170–570	Blood vessel	[21]
	Fibrinogen	HFP	120–610	Rat cardiac fibroblast	[151]
	Chitin	HFP	163–8770	Skin	[152]

Abbreviations: DMF: Dimethylformamide; DCM: dichloromethane; THF: tetrahydrofuran; HFP: 1,1,1,3,3,3-hexafluoro-2- propanol; TFE: 2,2,2-trifluoroethanol; HCL: hydrochloric acid; hMSC: human mesenchymal stem cells.

from the apex of the cone and accelerates towards the grounded collector [47]. Two different models were proposed to explain the nanofiber drawing process: single filament elongation or splitting of a fiber into several smaller fibers [48]. Many investigators supporting the single fiber theory reported that the fiber jet undergoes a chaotic whipping and bending trajectory while accelerating towards the collector due to repulsive interactions among like charges in the polymer jet [49,50]. This process aids in fiber thinning and solvent evaporation by increasing the transit time and path length to the collector. Doshi and Reneker hypothesized the occurrence of a different model involving the splitting of a fiber jet caused by the increase in charge repulsion during elongation [51]. However, recent studies have imaged the unstable zone of fiber jet with the aid of high-speed photography. These studies revealed that a whipping instability leads the single fiber to bend and turn rapidly, thereby resulting in the incorrect notion of fiber splitting [52,53].

With recent technical developments and a better understanding of the process, continuous fibers with diameters ranging from nanometers to a few micrometers have been generated by using a diversity of materials in various fibrous assemblies. Moreover, the simplicity of the setup makes the process highly attractive to both academia and industry [54]. In the basic process of electrospinning, a number of factors have been found to affect fiber formation and structure [18,38].

4.2. Process parameters for silk electrospinning

Factors that significantly affect the process of electrospinning have been widely investigated on a great number of polymers [55–58], and are summarized into three main categories:

(i) Substrate and solution related parameters, such as the chemistry, molecular weight and molecular weight distribution of the polymer, the rheological properties of the solution (concentration, viscosity, elasticity, conductivity, surface tension);
(ii) Process related parameters, such as hydrostatic pressure in the capillary tube, applied electrical potential, flow rate of the solution and distance from tip to collector;
(iii) Environment related parameters, such as temperature, humidity and air velocity in the electrospinning chamber.

An optimal combination of these electrospinning parameters should establish conditions to generate fibers with narrow variations in diameter and absence of beads.

4.2.1. Substrate-related parameters

The relationship between polymer concentration and fiber diameter has been discussed in many studies [59–64]. Generally, increasing the concentration of a polymer solution results in increased fiber diameter and decreased in bead formation, though the applicable ranges vary depending on the solvent system, average molecular weight and molecular weight distribution of the polymers used [65–67].

Polymer concentration and molecular weight collectively determine the 'spinnability' of the solution through effects on solution viscosity and surface tension [18]. If the solution is too dilute, the fiber will break into microsize droplets before reaching the collector as a result of varicose jet instability and the phenomenon of "electrospray" will be observed instead of "electrospinning". Electrospray is also observed when a polymer solution with low molecular weight is used. However, if the solution is too concentrated, it will be difficult for the polymer solution to flow through the capillary due to high viscosity, therefore no fiber will form. Ohgo et al. demonstrated the relationship between fiber characteristics and silk electrospinning solution in hexafluoroacetone (HFA) from different sources [68]. The concentration of silk in solution had a significant effect on nanofiber diameter. Continuous fibers were obtained only when a *Bombyx mori* silk (silkworm silk, domesticated source of silk fiber for the textile industry) solution higher than 2% (w/v) concentration was used. Fibers with the smallest mean diameter and narrowest distribution were observed from silk solution of 3% (w/v), compared to those from 5 and 7% (w/v) solutions (Fig. 2). When *Samia Cynthia ricini* silk and genetically engineered hybrid silk proteins were employed, the optimum conditions for fiber formation were found to be 10 and 12% solutions, respectively. This reveals the effect of silk sources on electrospinning processing parameters.

A similar effect of silk concentration on fiber formation was also observed when different solvent or aqueous systems were employed. However, the threshold of silk solution concentration versus spinnability varied significantly. Jeong et al. studied the effects of solvents (hexafluoroisopropanol (HFIP), formic acid) on diameter and secondary structure of the *B. mori* silk nanofibers [69]. They found the mean diameter of the electrospun nanofibers, composed of silk fibroin dissolved in formic acid, were smaller (80 nm) than those from (HFIP) (380 nm). This difference was due to the faster evaporation rate of HFIP than formic acid, which led to the formation of thicker fibers with less elongation. Faster evaporation of HFIP also led to a lower proportion of β-sheet in the nanofibers, based on Infrared (IR) and ^{13}C solid-state cross polarization (CP)/magic angle spinning (MAS) nuclear magnetic resonance (NMR) spectroscopy. Higher solvent volatility increased fiber porosity in other polymer system, but this has not been observed in electrospun silk fibroin nanofibers.

Wang et al. electrospun silk fibroin using an aqueous solution from *B. mori*, solving the potential concerns of chemical residuals from solvents [70,71]. Concentrated silk aqueous solution was needed in order to increase the solution spinnability. Fibers did not form when the aqueous silk solution at 17% (w/v) was used, while at 28% (w/v), silk fibers with diameters from 400 to 800 nm were observed, with circular cross-sections and smooth exterior surfaces. However, when the silk solution at 39% (w/v) was used, uneven and ribbon-shaped silk fibers were observed, likely due to the slow water evaporation from fiber surface before the fibers reached the collector (Fig. 3A). The rheological behavior of aqueous silk solutions was correlated to fiber morphology (Fig. 3B). The results revealed that silk solutions with viscosity lower than 40 mPa s did not provide sufficient molecular chain entanglements in solution to prevent the breakup of the electrically driven jet and led to electrospray. Jin et al. demonstrated the possibility of using a lower concentration of aqueous silk fibroin solution for electrospinning by blending with as little as 12% (w/w) poly(ethylene oxide) (PEO) [72]. From this blend, nanofibers with comparable diameters to a pure aqueous silk system were generated (approximately 750 nm), but more homogenous fiber diameters were observed with circular rather than ribbon-shaped cross-sections.

Electrospinning was employed as a technique to help with understanding the spinning process of native silk fibers by silkworms and spiders. The effects of solution pH on electrospun fiber morphology and properties was investigated, since a decrease in pH of the silk dope from 6.9 to 4.8 was observed during the native flow from the posterior division to the anterior division of a silkworm gland [73–75]. The results indicated that reduction of solution pH caused a decrease in the concentration of aqueous silk fibroin solutions that could be electrospun. Moreover, the average diameter and diameter distributions of the electrospun silk fibers became smaller and narrower due to the decrease in spinnable solution concentration. With the combined reduction in pH and concentration, the morphology of the electrospun silk fibers changed from ribbon-like to a uniform cylinder. An average diameter of 265 nm was obtained from 25% (w/v) silk fibroin solution at pH of 4.8. However, when electrospinning was performed using silk fibroin solution at pH 6.9, mimicking the posterior division of silkworm gland, only a solution greater than 33% (w/v) was capable of forming fibers. An average diameter of 850 nm was obtained under these conditions, which is smaller than native silk fibers (~15 μm).

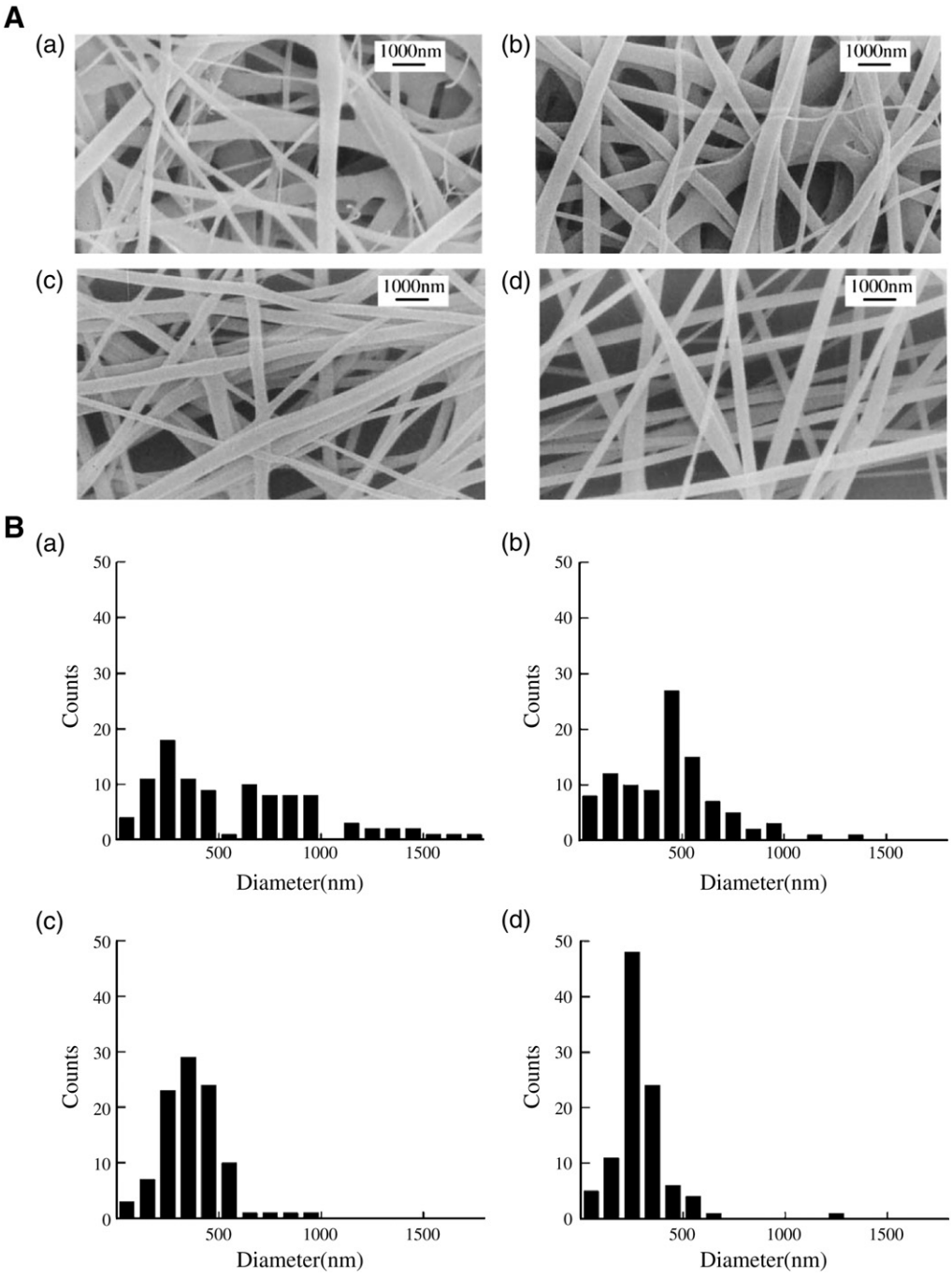

Fig. 2. Scanning electron micrographs (A) and distributions of diameters (B) of non-woven silk fibers from of non-woven silk fibers from (a) 7 wt.% silk/HFA solution, 1.3 kV/cm; (b) 5 wt.% silk/HFA solution, 1.6 kV/cm; (c) 5 wt.% silk/HFA solution, 1.0 kV/cm and (d) 3 wt.% silk/HFA solution, 1.0 kV/cm. (From Ref. [68] with permission).

Like most natural polymers, silk fibroin solution is regenerated from natural sources, such as silkworm cocoons and spider fibers. Thus, the molecular weight and molecular weight distribution can vary due to the differences in source and processing methods. However, most of the studies related to silk fibroin electrospinning have not considered the molecular weight and molecular weight distribution as factors in the process, and the relationship between molecular weight and the minimum spinnable solution concentration is undefined. The extent of polymer chain cleavage is determined by variables in the silk regeneration process, such as the strength and concentration of degummed chemicals, boiling time, and silk fiber dissolvation temperature and time. A summary of silk fibroin sources, process methods and electrospinning parameters can be found in Table 2.

4.2.2. Process-related parameters

Among the electrospinning process parameters examined, the applied electric potential had an effect on electrospinning in terms of fiber jet formation, bead defects and fiber diameter [61,76,77]. For example, fiber jets were induced when an electric field of 4 kV/cm was used to spin *B. mori* silk solution (8%, w/v) in formic acid, while fibers were not able to form when a lower electric field of 3 kV/cm was used [78]. This suggests that increased electrostatic forces can overcome solution surface tension and further extract silk fibroin chains. However, the tendency of the fiber jet to contract into droplets resulted in bead defects along the fiber extensions due to insufficient entanglement between silk macromolecules. Similarly, increased interactions between silk fibroin macromolecules were induced when increased electric potential was applied to a 17% (w/v) aqueous silk

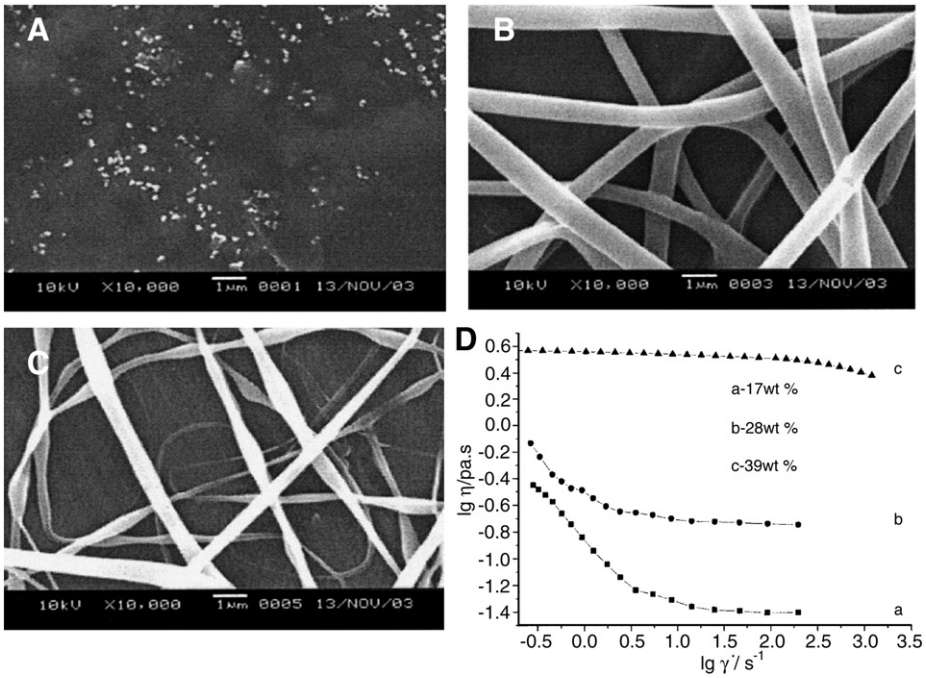

Fig. 3. Scanning electron micrographs of electrospun silk fibers with applied voltage at 20 kV and (A) 17%, (B) 28% and (C) 39%. (D) Rheological behavior of silk fibroin aqueous solutions with different concentrations. Scale bar = 1 μm. (From Ref. [70] with permission).

fibroin solution [70]. An increased electric field also resulted in less round and more ribbon-shaped fibers due to reduced time for water evaporation.

The effect of electric potential on fiber diameters was demonstrated in a variety of polymer systems. Generally, an increase in voltage results in an initial decrease followed by an increase in fiber diameter, while no significant effects were found when the increase of voltage was above a certain level [18]. Fiber diameter dependence on electric potential was observed in electrospinning of silk fibroin solutions (as shown in Fig. 4A) and in multiple solvents (HFA and formic acid) and aqueous systems [68,70,78]. Meechaisue et al. investigated the influence of voltage on electrospun fiber diameter using 40% (w/v) silk fibroin solutions regenerated from two distinct silkworm cocoons (indigenous Thai silkworms (Nang-Lai) and Chinese/Japanese hybrid silkworms (DOAE-7)) [79]. The results indicated that when the electric field was increased from 10 to 20 kV/cm the average diameter of electrospun fibers from DOAE-7 silk increased from 480 to 810 nm, while those from Nang-Lai silk increased from 440 to 610 nm. The increased fiber diameters resulting from the increased electrostatic fields were attributed to an increase in mass throughput with an increased electric force.

The flow rate of polymer solution, determined by the gravity or use of a pump, can also affect the size and shape of electrospun fibers [49,80,81]. The feed rate directly impacts the volume of solution suspended at the tip of the spinneret, which influences the shape of the Taylor cone. The maintenance of the cone shape at the tip of the capillary is important to obtain a continuous fiber jet [35]. Megelski et al. examined the effect of flow rate on the structure of electrospun polystyrene fibers in tetrahydrofuran (THF) solution [42]. Increases in fiber diameter, pore size, bead defects, and ribbon-shaped fiber formation have been demonstrated in response to increased flow rate. No systematic study involving the effect of flow rate on electrospun fiber characteristics has been conducted, though the general rule for other polymers should be applicable to silk fibroin protein. Generally, flow rates in the range of 1–4 mL/h have been used for silk fibroin electrospinning in various solvent/water systems. The optimal conditions can be achieved by controlling the shape of the Taylor cone without excess solution dripping.

The distance between the capillary tip and the collector can also influence the fiber diameter and morphology, however to a lesser extent than other process factors, such as electric potential and flow rate. It has been found that a minimum distance is required for fibers to have sufficient time to dry before reaching the collector. Otherwise, 'electrospray' will occur instead of 'electrospinning'. Bead formation was observed at distances that were either too close or too far from capillary tip to collector [82,83]. The spinning of 9% (w/v) regenerated *B. mori* silk solution at an electric field of 3 kV/cm was carried out at three different distances (5, 7 and 10 cm), and reduced fiber diameters were observed with increased distance [78]. Sukigara et al. [84] also observed an increase in fiber diameter in response to decreased spinning distance from 7 to 5 cm during spinning a silk solution at concentrations of 10–18% (w/v). However, when a higher concentration (20% w/v) was employed at less than 4 kV/cm, a decrease in fiber diameter was observed. This reflects the dependence of the relationship between spinning distance and diameter on solution concentration and electric field (Fig. 4B).

On the basis of experimental studies, mathematical models were also used to determine the relationship between electrospinning parameters (silk fibroin concentration, electric field and spinning distance) and fiber diameters, predicting the optimal conditions for electrospinning of silk fibroins [78,84]. Sukigara et al. initially employed 'two-way analysis' to study the influence of electric field and spinning distance on electrospun fiber diameter from *B. mori* silkworm [78]. However, no significant difference in fiber diameter was found when spinning of 15% (w/v) silk fibroin solution at a spinning distance between 7 and 10 cm in a fixed electric field. An exponential relationship between silk concentration and fiber diameter was observed regardless of the electric field applied in the range of 2–4 kV/cm. Following this preliminary work, an alternate mathematical method, response surface methodology (RSM), was employed to model the process conditions and establish a quantitative basis for the relationships between electrospinning parameters and the resulting fiber diameter [84]. Since RSM takes the combined effects of several parameters into account and uses statistical methods to fit an empirical model to the experimental data, the important

Table 2
Related parameters for electrospinning silk fibroin.

Authors [reference]	Silk type	Silk processing		Concentration (wt.%)	Solvent	Fiber diameter (nm)	Voltage (kV)/ electric field (kV/cm)	Distance (cm)	Flow rate (mL/min)
		Degum (boiling)	Dissolvation						
Zarkoob et al. [153]	*Nephila clavipes* dragline silk	N/A	HFIP, 20 min	0.23–1.2	HFIP	8–200 (median = 100)	24–30 kV	15	
	B. mori cocoon silk	No	HFIP, 5 month	0.74	HFIP	6.5–100 (median = 25)			
Jin et al. [137]	*B. mori* cocoon silk	0.02 M $NaCO_3$, 30 min	9.3 M LiBr, 60 °C	8	PEO/H_2O	700 ± 50	0.6 kv/cm	20	0.02–0.05
Wong Po Foo et al. [154]	Spider silk–silica fusion proteins	N/A	HFIP	2	HFIP		15–20 KV		0.01
Ohgo et al. [68]	*B. mori* cocoon silk	0.5% (w/v) Marseilles soap, 30 min (3x)	9 M LiBr, 40 °C	3, 5 and 7	HFA	100–1000	1–1.6 kV/cm	10–15	
	Samia cynthia ricini silk	0.5% $NaCO_3$, 30 min (5x)		10	HFA	<500	1 kV/cm		
	Recombinant hybrid silk of *B. mori* and *S.c.richni*	N/A		12	HFA	<500	1 kV/cm		
Sukigara et al. [84]	Degummed *B. mori* silk fibroin fiber	N/A	50% $CaCl_2$	10, 12,15 and 20	Formic acid (98–100%)		2–5 kV/cm	5 or 7	
Kim et al. [90]	*B. mori* cocoon silk	0.5 %(w/w) $NaHCO_3$, 30 min (2x)	$CaCl_2$/CH_3CH_2OH/ H_2O (1/2/8 in mole), 70 °C, 6 h	6–15	Formic acid (98%)	30–120 (mean = 80)	15 kv	7	0.025
Min et al. [131]	Degummed *B. mori* silk yarn	N/A	$CaCl_2$/CH_3CH_2OH/ H_2O (1/2/8 in mole), 70 °C, 6 h	7	HFIP	250–530 (mean = 380)	2 kV/cm	8	2
Wang et al. [70]	*B. mori* cocoon silk	0.5% (w/w) $NaHCO_3$, 30 min (2x)	9.3 M LiBr, RT	17, 28 and 39	H_2O	100–1000 (mean = 700)	10–40 kV	12	
Ayutsede et al. [85]	Degummed *B. mori* silk fiber	N/A	50% $CaCl_2$	9 and15	Formic acid	2–400 nm (mean = 60)	2–3 kV/cm	5, 7 or 10	
Jeong et al. [94]	Degummed *B. mori* silk fiber	N/A	$CaCl_2$/CH_3CH_2OH/ H_2O (1/2/8 in mole), 70 °C, 6 h	7	HFIP	250–550 (mean = 380)	2 kV/cm	8	2
Kang et al. [106]	*B. mori* cocoon silk	0.02 M $NaCO_3$, 30 min	9.3 M LiBr, 60 °C	8	PEO/H2O	460 ± 40	12 kV		0.02
Zhu et al. [73]	*B. mori* cocoon silk	0.5 wt.% $NaCO_3$, 30 min	9.0 M LiBr, 40 °C, 2 h	30, 33 and 38	Citric acid–NaOH–HCl	1500–2500 (mean = 1700)	20, 30, 40 kv		0.033
Baek et al. [141]	Degummed silk fiber	N/A		12	Formic acid (98%)	170–250	12 kV	10	
Silva et al. [155]	*B. mori* cocoon silk	1.1 g/L $Na2CO_3$, 1 h, 0.4 g/L $NaCO_3$,30 min	9.3 M LiBr, 65 °C	12	Formic acid (99%)	140–590	21 kV	10	0.005
Zhou et al. [156]	Spider silk	N/A		11	Formic acid	200–1200	15–30 kV	15	0.06–0.09

parameters can be represented in a simple and systematic way and to predict the results of experiments with different parameter combinations. Two second-order equations were fit for the natural logarithmic fiber diameter using RSM at spinning distances at 5 and 7 cm. The results indicated that fiber diameter was more responsive to electric field variations at low concentrations and that lower silk fibroin concentrations result in smaller fiber diameters.

Also, fiber diameter decreased as the electric field increased, as observed from contour plots for both 5- and 7-cm spinning distances at a fixed silk concentration. Similar to the experimental results, mathematical results also supported the concentration-dependent effects of spinning distance on fiber diameter. Therefore, response surface methodology provides a more comprehensive prediction tool than two-way analysis for identifying the processing window suitable for producing nanoscale fibers.

In summary, the effects of substrate- and process-related parameters on fiber jet formation and the resulting electrospun fiber characteristics, such as diameter, cross-section and bead defects are complex and inter-related. In particular, the effects of solution properties can be difficult to isolate since varying one parameter will change others. Additionally, the dominant effects among these parameters can shift from one to another depending on the specific parameter combinations. Recent advances in experimental studies have elucidated some of the connections between electrospinning factors (applied electric field, spinning distance and solution properties) and fiber properties, as summarized in Table 2. However, limited information is still insufficient for future process prediction and control due to the assortment of combinations. Mathematical modeling may be a useful tool for separating variable interactions and determining co-dependencies.

4.3. Post treatment

The major conformations of electrospun silk fibroin nanofibers are random coil, α-helix (silk I) and β-sheet (silk II) [85]. The crystallization (conversion of random coil and helices into the stable β-sheet conformation) can be induced by physical (thermal) [86] or chemical (e.g., methanol) [87] treatments. Matrix treatments using organic solvents such as methanol are highly effective and the most common option for crystallization [88,89]. Kim et al. investigated the efficiency of using 50% (v/v) aqueous methanol solution to treat electrospun silk fibroin with varied times (10 to 60 min) at room temperature [90]. A strong β-sheet characteristic peak was found from methanol-treated electrospun silk nanofibers by frustrated total internal reflection (FTIR), X-ray diffractometry and solid-state ^{13}C NMR, irrespective of treatment time. The results indicated that the conformational transition of the

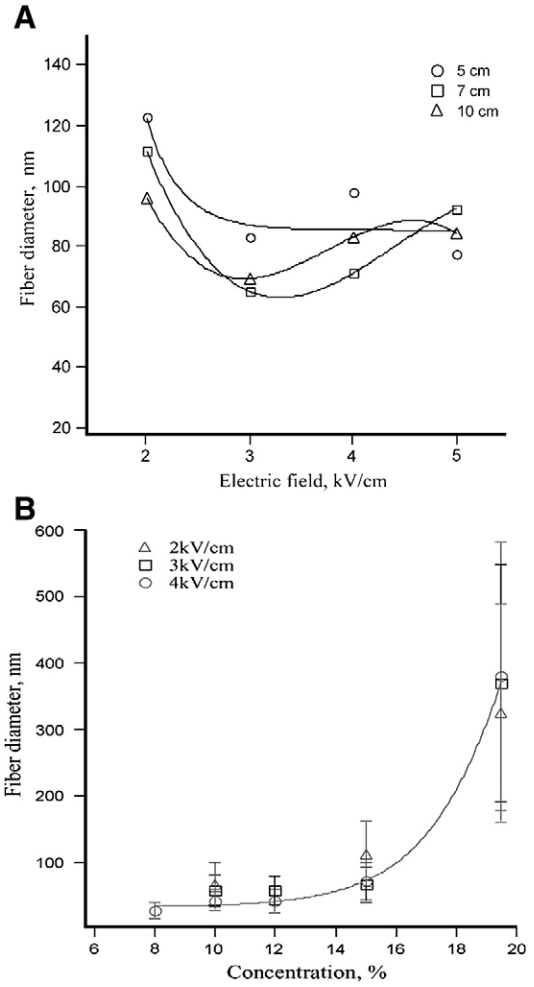

Fig. 4. Effects of electrical field, polymer concentration and spinning distance on electrospun silk fiber diameter. (A) The relationship between fiber diameter and electrical field with concentration of 15% at spinning distances of 5, 7 and 10 cm. (B) The relationship between fiber diameter and silk concentration at three electric fields (2, 3, 4 kV/cm) with fixed spinning distance. (From Ref. [78] with permission).

unmodified silk fibroin nanofibers to crystalline structure was rapid and almost completed within 10 min. Additionally, the porosity of silk nonwoven matrices decreased from 76.1% to 68.1% after methanol treatment for 60 min and the corresponding total pore volume decreased from 2.017 to 1.395 mL/g. This indicates fiber shrinkage caused by the methanol treatment, an expected result from the dehydration effects of this solvent.

Methanol-treated silk fibroin matrices are often brittle due to their high crystalline content. An alternate method, water-based annealing, has been tested for its effectiveness for preparing water-stable silk fibroin matrices [91,92]. Min et al. reported the differences of electrospun silk fibroin matrices after treatment with either aqueous methanol solution (50%) or water vapor with varied treatment times [93]. Similar weight losses at about 15% (w/w) were found for both treatment methods, while the non-treated silk fibroin matrices lost about 35% (w/w). However, a longer time was required for water vapor treatment at low temperature (at least 1 h) versus methanol treatment (<10 min) in order to complete the conformational transition. Both treatments led to significant increases in yield stress, elongation at break and tensile modulus for electrospun silk nanofibers compared to non-treated samples. However, water vapor treatment yielded different mechanical properties compared to methanol treatment. Methanol-treatment provided the higher yield stress and tensile modulus, while water-vapor treatment provided better elastic properties. These differences were attributed to the lower β-sheet content in water-vapor-treated silk nanofibers (47%) compared to that in methanol-treated nanofibers (74%). Water vapor annealing also improved the biocompatibility of electrospun silk matrices versus methanol treatment, with enhanced adhesion and spreading of human keratinocytes and fibroblasts.

In addition to the above two common methods for silk fibroin crystallization, the efficiency of solvent (ethanol, methanol and propanol) vapors in inducing conformational transitions of silk nanofibrous matrices was compared to that of water vapor treatment with time [94]. Based on IR spectra, the area ratios of silk II and silk I structures (A_{II}/A_I) in the amide I region of silk fibroin nanofibers were used to compare the structural changes caused by different solvent vapors at 35 °C. The conformational transition induced by the various solvent vapors reached equilibrium in approximately 30 min, and the degree of transition from silk I to silk II (A_{II}/A_I) was strongly dependent on the solvent used, with methanol > water > ethanol > propanol (Fig. 5A). The conformational transitions induced by water vapor were also affected by temperature. Increasing temperatures increased β-sheet content at a low temperature range (25–45 °C) or reduce the time to reach transition equilibrium at a high temperature range (45–55 °C) (Fig. 5B).

Thus, methanol solution/vapor and water vapor are the most effective treatments for the crystallization of electrospun silk matrices, although the selection of post-treatment methods should consider the matrix properties for specific applications.

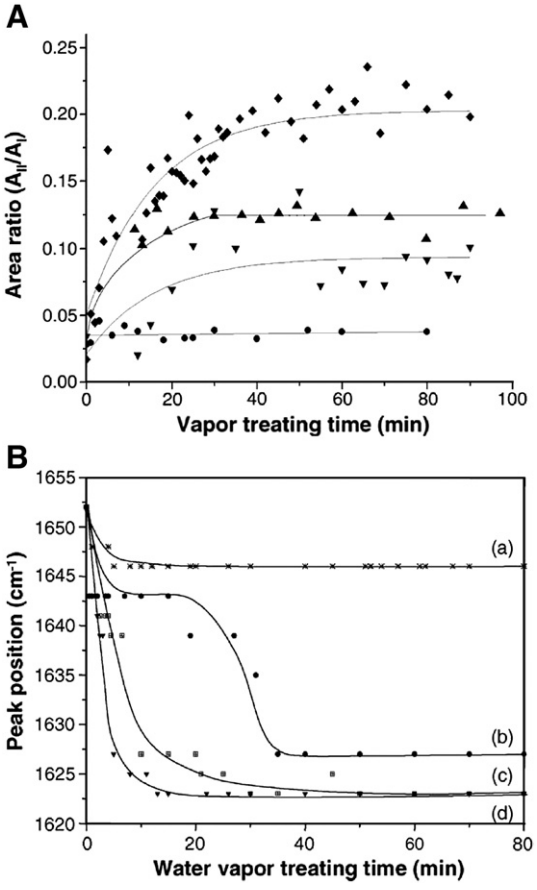

Fig. 5. Effects of different solvent vapor treatment and temperature on conformational change of silk nanofiber. (A) Changes of area ratios of silk II and silk I structures (A_{II}/A_I) of the amide I region of silk nanofibers, determined from IR spectra during solvent vapor treatments at 35 °C ((▲) water; (♦) methanol; (▼) ethanol; (●) propanol). (B) Changes in peak position of amide I band (β-sheet conformation) of regenerated silk nanofibers treated with water vapor at: (a) 25 °C, (b) 35 °C, (c) 45 °C, and (d) 55 °C. (From Ref. [94] with permission).

4.4. Composite nanofibers

Composite materials are often desirable in order to achieve combined properties from the constituent materials. Composite electrospun nanofibrous matrices can be obtained by either spinning polymer blends using a single needle or a side-by-side configuration (Fig. 6A). The side-by-side configuration is very useful when the polymers of interest are not soluble in a common solvent [95]. Park et al. successfully electrospun a series of chitin/silk fibroin mixtures at different ratios under the same processing conditions [96]. The average diameters of chitin/silk fibroin blend fibers were found to decrease from 920 to 340 nm with increased chitin content ranging from 25% to 75% (w/w). The authors attributed the gradual decrease in fiber diameter with increased chitin concentration to the increase in solution conductivity due to the higher polarity of chitin. Moreover, the hydrophilicity of the chitin/silk blend nanofibers after water vapor treatment was improved by increasing the chitin fraction. Recently, Yoo et al. electrospun chitin/silk 'hybrid matrices' at different weight ratios using a side-by-side configuration [97]. Higher water uptake was demonstrated for chitin/silk blend matrices, compared to chitin/silk hybrid matrices of equal compositions. Furthermore, enhanced attachment and spreading of human epidermal keratinocytes was observed on chitin/silk blend matrices compared to hybrid matrices. This may have been caused by the variation in hydrophilicity of chitin/silk fibroin biocomposite matrices. Collagen/silk fibroin blend solutions in HFIP were electrospun into fibers, but no significant difference was found in average diameters regardless of the mixing ratio. Diameters ranged from 320 to 360 nm, with a relatively uniform distribution [98].

A coaxial nozzle configuration has also been used for electrospinning, which allows for simultaneous coaxial spinning of two different polymer solutions, leading to a core–shell morphology of fibers (Fig. 6B). Wang et al. successfully encapsulated a silk fibroin core fiber within a poly(ethylene oxide) (PEO) shell fiber [99]. The influence of process parameters, such as flow rates, on the fiber morphology was explored by varying the combinations of outer (shell) and inner (core) fluid flow rates in the range of 0.01 to 0.05 mL/min and 0.001 to 0.008 mL/min. The results indicated that increased inner or outer flow rates led to increases in corresponding fiber diameters. However, the shell diameter changed only slightly when the inner fluid (silk fibroin) flow rate was increased 5-fold. The inner flow rate is critical: either too low or too high of a flow rate will cause problems for silk fibroin encapsulation. When the rate is too low, no continuous silk fiber can form due to an insufficient supply of solution to form the core. When the inner fluid flow rate is too high, the silk solution cannot be entrained within the PEO solution, causing spraying to occur. The results indicated that a uniform, continuous silk fibroin (core)/PEO (shell) fiber can be obtained with the ratio of outer and inner flow rates in the range of 6:1 to 10:1. Also, the ratio of the cross-sectional area of the outer fiber to that of the inner fiber increased linearly with the increase of the flow rate ratio within this range. After water vapor treatment, PEO was extracted in water and solid, crystallized silk fibers with diameter as small as 170 nm were obtained. Thus, a coaxial nozzle configuration of electrospinning is valuable for generating of small diameter fibers with minor variation due to the constriction of shell fiber. In addition, this configuration is effective for generating fibers from individually unspinnable polymers.

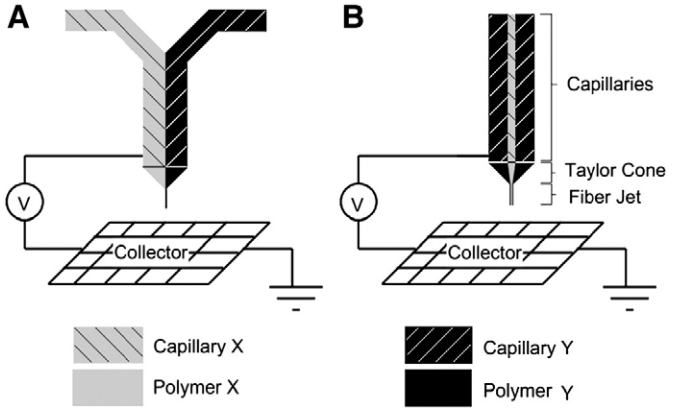

Fig. 6. Schematic of (A) side-by-side and (B) coaxial nozzle configurations. (From Ref. [18] with permission).

Composite electrospun nanofibers have been generated using different spinning configurations and provide diverse properties in terms of mechanical behavior and cell responses. However, further exploration of the process of composite nanofiber generation is needed in order to better understand the underlying mechanisms.

4.5. Three-dimensional (3-D) electrospun silk scaffolds

Electrospinning usually produces nonwoven sheets with a 2-D profile because of the required relatively low polymer solution ejection rate. Theoretically, 3-D nonwoven fibrous meshes can be obtained if the electrospinnng time is increased. However, the ability to continuously accumulate polymer fibers into a 3-D construct is hindered by the reduced conductivity of the collector during fiber accumulation. Ki et al. have successfully developed a sponge-like 3D nanofibrous matrix using a modified electrospinning method [100]. In this method, a coagulation bath filled with methanol was used as a collector instead of traditional flat or drum collector. A porogen, NaCl particles of 300–500 μm, was added to the electrospun silk fibroin nanofiber dispersion. After salt leaching, dual-porosity silk nanofibrous scaffolds were generated. The scaffolds exhibited a 3-D structure with nano-sized pores at the interstices of the entangled fibers and micro-sized (586–931 μm) pores formed by the salt particles (Fig. 7). The advantages of 3-D silk fibroin nanofibrous scaffolds for cell attachment and proliferation was also demonstrated when compared to 2-D silk fibroin electrospun sheets.

5. Functionalized electrospun silk matrices

To date, unfunctionalized electrospun matrices have been employed for tissue engineering applications. Current technological advances in electrospinning have enabled the development of 'functionalized' nanofibrous matrices able to release combinations of molecules including antibiotics, proteins, small molecules, and DNA. Drug loading is typically achieved through three methods [101]: (i) pre-spinning embedding bioactive agents in nanofibrous matrices by mixing with polymer solutions; (ii) post-electrospinning covalently conjugating or coating nanofibrous matrices with bioactive agents; or (iii) encapsulating bioactive agents in the core of fibers with core–shell structure through coaxial electrospinning.

Functionalized electrospun matrices have been developed and used as drug carriers and cell-culture scaffolds. As drug carriers, functionalized matrices improve therapeutic efficacy and safety through local delivery [102]. When employed for cell culture or tissue regeneration, functionalized matrices with drug release properties offer improved biocompatibility and can induce specific biological responses, ranging from decreased inflammation to increased cellular proliferation, migration, and differentiation. The electrospinning process provides flexibility in material selection, bioactive agent loading and delivery. Both biodegradable and non-biodegradable materials can be used for drug delivery and release may occur through diffusion alone or simultaneous diffusion and scaffold degradation.

Silk electrospun matrices have been functionalized with bioactive agents to improve drug activity and cellular responses. Lee et al. immobilized α-chymotrypsin (CT) on silk fibroin electrospun nanofibers with amino group pre-activation by glutaraldehyde [103]. A significant increase in enzyme loading efficiency was observed with

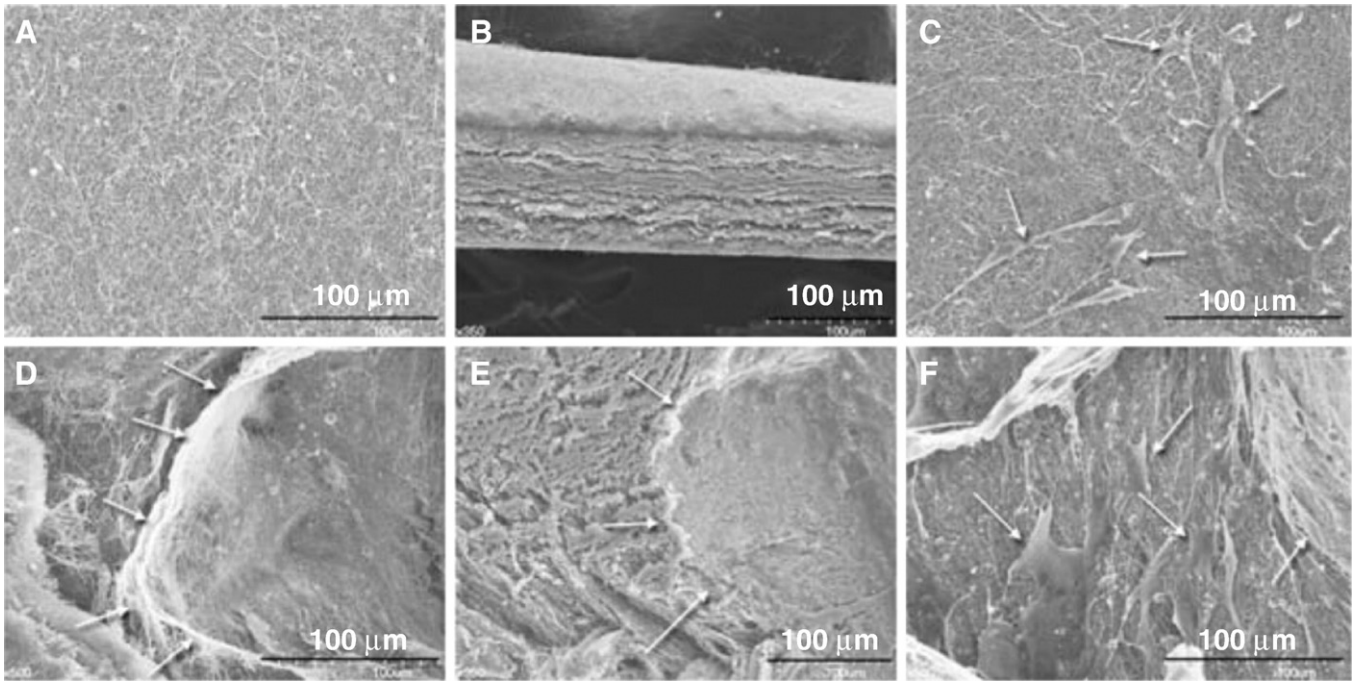

Fig. 7. Scanning electron micrographs of osteoblast attachment on (A–C) 2-D and (D–F) 3-D silk nanofibrous scaffolds 1 day after cell seeding. Scale bar = 100 μm. Arrows indicate pores and cells in the scaffolds. (From Ref. [100] with permission).

electrospun nanofibers from 8% (w/w) silk fibroin solution (SF8) (56.6 μg/mg), compared with silk fibroin microfibers (8.05 μg/mg) or cellulose fibers (1.8 μg/mg). The activity of immobilized CT on SF8 was almost 8 times greater than that on silk microfibers, due to the increased content of immobilized enzyme on SF8 and a superior microenvironment for enzyme stability. This could be attributed to a reduced surface area to volume ratio found in fibers with increased diameter resulting from higher silk concentrations. When the enzyme activity of immobilized CT on nanofibers constructed from varying silk concentrations were compared, a decreased amount of enzyme was observed on nanofibers electrospun from higher silk concentrations, but a significant difference was only observed between SF8 and SF11 (silk fibers from 11% w/w solutions). The loss of enzyme activity on SF11 was attributed to its multipoint attachment to the matrix, which restricted the conformational change and decreased the activity of enzyme, despite increasing stability. Immobilized CT on SF8 also exhibited significantly higher thermal stability compared to enzyme on SF11 or free CT, and retained more than 90% of its initial activity after 24 h at 25 °C. Significant improvement of enzyme stability in ethanol was also observed for immobilized CT on silk fibers compared to free CT. For example, 45% of initial enzyme activity on SF11 was retained after one-hour ethanol exposure compared to only 5% in free CT.

Li et al. incorporated bone morphogenetic protein-2 (BMP-2) into silk fibroin nanofibers by directly mixing into the spinning solution [104]. BMP-2 encapsulated in the silk fibroin matrices increased calcium deposition and decreased the proliferation of human bone marrow-derived mesenchymal stem cells (hMSCs), when compared with unfunctionalized silk fibroin matrices (control). Moreover, the BMP-2 resulted in enhanced expression of bone-specific markers at transcript levels compared to controls, indicating that electrospun silk nanofibrous matrices are an efficient delivery system for BMP-2. Improved bone formation, as indicated by increased calcium deposition and BMP-2 transcript expression, were also observed when nanoparticles of hydroxyapatite (nHAP) were incorporated into the silk electrospun matrices (Fig. 8). Furthermore, the coencapsulation of

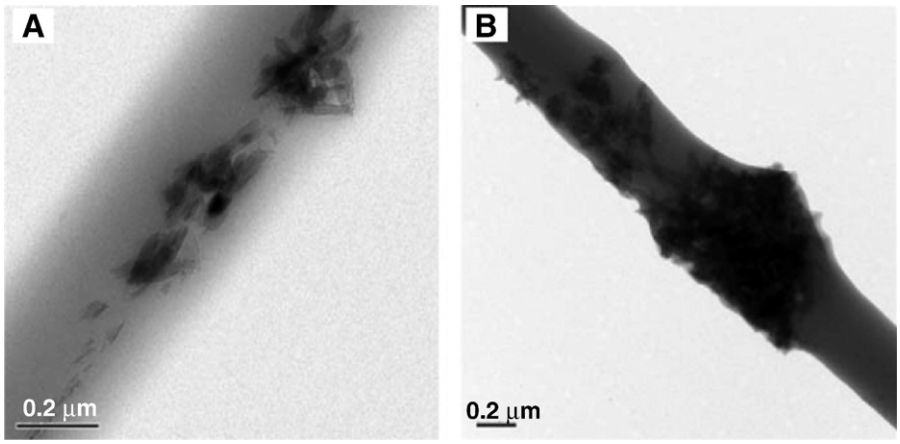

Fig. 8. TEM images of electrospun silk/nHAP fibers. Scale bar = 0.2 μm (From Ref. [104] with permission).

BMP-2 and nHAP in the electrospun silk fibroin matrices demonstrated greater bone formation when compared to singular component encapsulation or controls. Thus, mild aqueous process for silk fibroin electrospinning preserved the activity of BMP-2 and was a practical option for bioactive agent delivery, such as labile cytokines and morphogens.

Silver nanoparticles were incorporated on the surface of silk electrospun matrices to develop antimicrobial wound dressings [105]. Matrices with average fiber diameter of 460 nm were electrospun from an aqueous *B. mori* fibroin solution. Silver nanoparticles were incorporated by dipping the silk matrices into an aqueous silver nitrate ($AgNO_3$) solution followed by photoreduction. Binding of silver nanoparticles on the silk nanofibers was confirmed with field emission scanning and transmission electron microscopies. The interaction between silver nanoparticles and the amide groups in silk was confirmed by X-ray photoelectron spectroscopy.

In addition to biological functionalization, electric property modifications have also been examined in silk electrospun matrices multiwall carbon nanotubes (MWCNTs) [106]. Absorption of MWCNTs was carried out by dipping silk matrices into a MWCNT dispersion bath for 60 s, followed by rinsing in deionized water and drying under vacuum conditions. Triton X-100 surfactant was employed to disperse the purified MWCNTs to avoid aggregation, and dense absorption of MWCNTs was observed by scanning electron microscopy (Fig. 9). A significant amount of MWCNTs remained on the surface of nanofibers even after sonication, indicating the tight binding between MWCNTs and silk nanofibers. The electrical conductivity of the MWCNT-absorbed silk matrices increased to 2.4×10^{-4} S/cm at room temperature, while that of pure silk was 4.4×10^{-15} S/cm. The electrical conductivity remained constant regardless of extended dip-coating time (over 60 s), confirming the high absorption rate of MWCNTs on the surface of silk fibers. This high absorption rate was due to the interaction between the oxidized groups of MWCNTs and the peptide groups of silk fibroin molecules.

Silk electrospun matrices can be functionalized in a number of ways utilizing drugs, enzymes, growth factors, compounds, and conductive materials. Future research involving electrospun fiber functionalization lies in combining biological assays with chemical characterization to assess cellular responses. Also, a full understanding of delivery mechanisms involved with these matrices would be valuable to improve matrix designs, increase safety and efficiency of drug release, and provide a more tunable, controllable delivery system.

6. Tissue engineering application

Cells in human tissues and organs deposit their extracellular matrix in the form of nanoscale fibers, despite variation in chemical composition and mechanical characteristics. Blood vessels, skin, cartilage and bone are all characterized by well-organized hierarchical fibrous structure but with tissue/organ-specific arrangements [107]. However, this organ-dependent diversity has been understudied for fibrous matrices applied to tissue engineering. Still, a number of natural and synthetic biomaterials have been successfully electrospun and may eventually prove useful in addressing diverse requirements, such as mechanical properties and structural arrangements. These

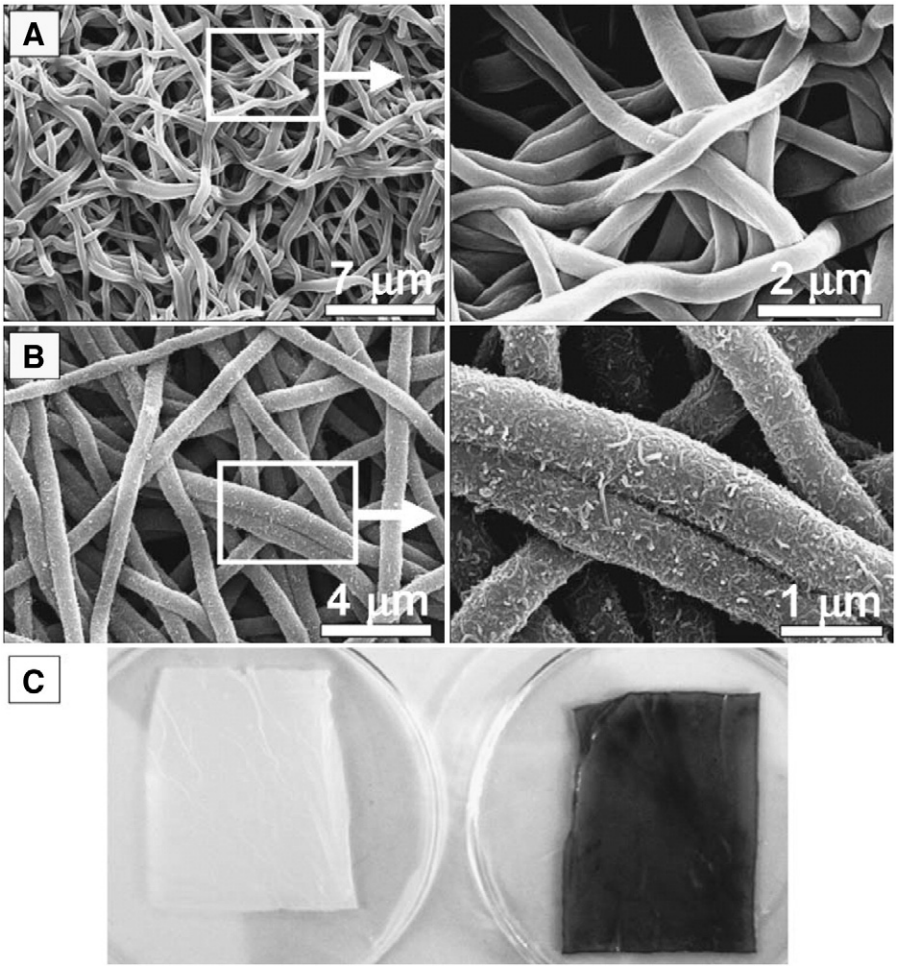

Fig. 9. SEM images of crystallized and PEO-extracted electrospun silk nanofibers (A) before and (B) after the adsorption of the MWCNTs. (C) macroscopic images of non-woven silk membrane before (left) and after (right) adsorption of the MWCNTs. (From Ref. [106] with permission).

materials have been spun into nano- and submicron-fibers and their potential for different tissue regeneration applications are being examined [108–116]. Natural polymers are often preferred due to their enhanced biocompatibility and biofunctional motifs [117]. Their similarity to native ECM components, such as collagen, hyaluronic acid and elastin, provide advantages through chemical signaling. Collagen is the most commonly used natural material due to its prevalence in the ECM of diverse tissue types. However, *in vitro* collagen does not provide sufficient mechanical strength and degradation is too rapid, limiting applicability for tissue regeneration. Mechanical weakness and accelerated degradation are also concerns for other natural biomaterials, including hyaluronic acid, gelatin and alginate.

Silk fibroin biomaterial in various formats has shown good biocompatibility, slow and controllable degradability, and minimal inflammatory response [21,23,118,119]. Furthermore, the excellent mechanical properties of silk fibroin make it a unique natural polymer. Silk fibroin matrices in the form of electrospun nanofibers have demonstrated potential in various tissue regeneration/repair applications.

6.1. Vascular grafts

Over the last 50 years, many attempts have been made to develop small-diameter blood vessels due to increased demands for vessel transplants, but almost of these approaches all have encountered failure. Greatly reduced graft patency was observed when cell-free synthetic prostheses were utilized for small diameter arteries, such as coronary and infragenicular vessels [120–123]. Attention to tissue engineered vascular grafts has increased due to the inclusion of vascular cells. Electrospun silk matrices have potential as vascular graft matrices due to their ability to support the attachment, proliferation and differentiation of vascular cells and resist shear stress and pressure from simulated blood flow.

Bondar and colleagues have investigated endothelial cell (EC) responses to nano- and micro-scale silk fibers in terms of cell morphology, proliferation, formation of intercellular contact, and expression of adhesion molecules [124]. Fully developed intercellular contact between ECs on the nano- and micrometric matrices was detected by identifying platelet/endothelial cell adhesion molecule-1 (PECAM-1) and vascular endothelial cadherin (VE-cadherin) protein expression using immunocytochemistry. The mRNA transcript levels of these adhesion molecules revealed no significant differences between micro- and nanofibrous scaffolds. Also, interactions between ECs and silk matrices were investigated through the expression of specific transmembrane receptor molecules such as integrins. The results of real-time PCR revealed significant upregulation of integrin-β1 in ECs grown on nanofibrous compared to microfibrous scaffolds. In addition, the formation of new focal adhesions (FAs) and polarization at the leading edge indicated a stronger migratory state of ECs on nanofibrous rather than microfibrous matrices. The authors attributed this to increased integrin expression, which may activate signal transduction to increase FAs, cell attachment, polarization and hence migration.

Soffer et al. [125] successfully electrospun silk into tubular structures with an inner diameter of ~3 mm and an average wall thickness of 0.15 mm (Fig. 10A). An average ultimate tensile strength (UTS) of 2.42 ± 0.48 MPa and a linear modulus of 2.45 ± 0.47 MPa were obtained. These results were comparable to those from a previous study of silk electrospun mats by Ayutsede et al. [85]. The average burst strength of the tubular scaffolds was 811 mmHg (Fig. 10B), which is greater than values from graft scaffolds prepared with collagen (71 mmHg) or other commonly used natural biomaterials [126]. However, further development is needed to reach the gold standard of the saphenous vein whose burst strength is 1800 mmHg [127].

Following Soffer's work, the evaluation of the biological potential of these electrospun silk matrices for vascular tissue engineering was determined [21]. The proliferation, metabolic viability, morphology and phenotype of human aortic endothelial cells (HAECs) and human coronary artery smooth muscle cells (HCASMCs) on 2-D electrospun silk matrices were examined. Good retention of vascular cells was demonstrated; cell numbers remained high for HCASMCs over 36 days

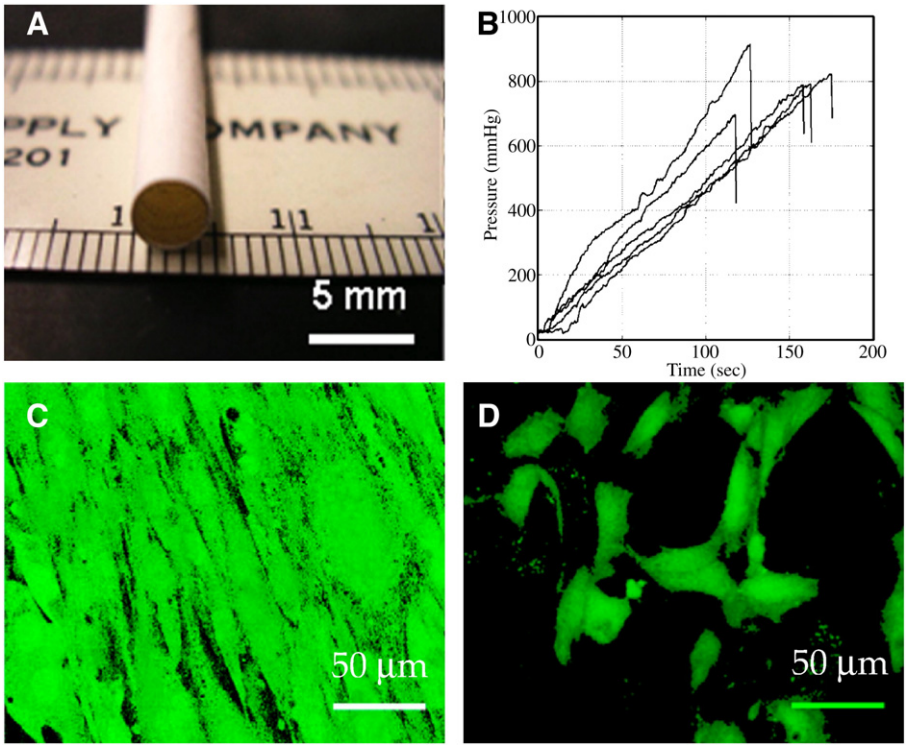

Fig. 10. (A) Macroscopic image of tubular electrospun silk fibroin scaffold. (B) Internal pressure change of tubular scaffold as function of time. (C) Smooth muscle cell and (D) endothelial cell morphology on the electrospun silk mats stained with Live/Dead kit. (From Ref. [125,21] with permission).

and HAECs over 14 days in culture with high seeding density. The maximum metabolic activity of HCASMCs and HAECs was observed around days 10 and 14, respectively. HCASMCs transformed from a stellate morphology and random orientation to a spindle shape with parallel alignment by day 5, and enhanced elongation was exhibited on day 10. Morphological change of HAECs was also observed with the formation of a short cord-like structure on day 4, and a complex interconnecting network of capillary tubes with lumens from day 7 to 14 (Fig. 10C). The phenotypes of both vascular cell types were further assessed using phenotype-specific protein markers. Positive staining of smooth muscle α-actin (SM-actin) and smooth muscle myosin heavy chain 2 (SM-MHC2) for HCASMCs, as well as CD146, VE-cadherin and PECAM-1 for HAECs was identified. Furthermore, expression of the major ECM components of vessel walls (collagen I and elastin) was demonstrated at both protein and transcript levels for HCASMCs, indicating the SMC functionality on electrospun silk matrices. Thus, the potential of electrospun silk scaffolds for vascular tissue engineering application was demonstrated for both biological and mechanical needs. Future work with silk electrospun small-diameter vascular grafts will need to focus on co-cultures of endothelial and smooth muscle cells in a tubular, perfusion environment to more closely mimic the *in vivo* environment.

6.2. Skin tissue

Skin plays a crucial role in protecting the human body against the environment, dehydration, and infectious agents. Skin cells located in two main layers: a keratinized, stratified epidermis and an underlying thick layer of collagen-rich dermal connective tissue. Loss of large portions of skin integrity from burns, wounds, or disease may result in significant disability or even death. However, skin replacement has been a challenging task for surgeons because of transplant limitations. Tissue-engineered skins provide an option to treat skin loss in many different forms: autologous and allogenic keratinocyte grafts, acellular biological matrices and cellular matrices including biological substances [128].

Min and colleagues carried out a series of studies to investigate the potential of silk electrospun matrices for accelerating early stages wound healing [129–131]. The adhesion and spreading of normal human keratinocytes and fibroblasts on methanol-treated silk fibroin nanofibers alone or precoated with ECM proteins (collagen type I, fibronectin and laminin) was evaluated. For keratinocytes, but not fibroblasts, coating with collagen I promoted cell adhesion and spreading. Laminin coating stimulated cell spreading, but not cell attachment. Cell adhesion and spreading on fibronectin-coated silk matrices was found comparable to that on BSA-coated matrices [129]. In wound healing studies with electrospun silk nanofibers, microfibers, and films [130], nanofibrous matrices promoted human oral keratinocyte adhesion and spreading, especially when a collagen type I coating was included. The authors attributed the results to the higher surface porosity and surface area-to-volume ratio of nanofibers, which formed a higher surface area for cell attachment. Fibroblast spreading was significantly improved when silk matrices were treated with water vapor rather than methanol [131]. Thus, electrospun silk nanofibrous matrices treated with water vapor followed by collagen I coating was the best candidate for a skin tissue template or wound dressing.

In another study, chitin was blended with silk fibroin to fabricate composite fibrous scaffolds for skin tissue engineering, due to the wound healing effects of chitin [132]. The chitin/silk fibroin blends at varied ratios were electrospun into nanofibrous matrices and evaluated for initial cell attachment and spreading [133]. Increased adhesion of keratinocytes was observed on chitin/silk blend matrices compared to pure chitin matrices, although there was no difference for fibroblasts. Chitin/silk blend nanofibrous matrices containing 75% chitin and 25% silk fibroin (75%/25%) gave the greatest cell spreading for keratinocytes and fibroblasts. Yoo et al. fabricated chitin/silk hybrid matrices at various blend ratios using side-by-side electrospinning and compared these to chitin/silk blend matrices for keratinocyte adhesion and spreading [134]. Chitin/silk blend matrices (75%/25%) demonstrated higher support for adhesion and spreading than all chitin/silk hybrid matrices, thus demonstrating the strong potential of blend matrices as skin regeneration substitutes (Fig. 11).

Yeo et al. investigated the potential of collagen/silk blend electrospun matrices for skin tissue engineering [98]. Surprisingly, pure collagen and pure silk fibroin matrices exhibited better results in terms of human keratinocyte attachment and spreading than collagen/silk blend or hybrid matrices irrespective of the mixing ratios. On the other hand, all matrices had similar effects on human fibroblast attachment and spreading. When collagen/silk hybrid matrices and collagen/silk blend matrices with equal component ratios were compared, hybrid matrices consistently supported better cell attachment and spreading.

6.3. Bone

Bone tissue is a specialized form of connective tissue, which is composed of calcified extracellular matrix and bone cells including osteoprogenitor, osteoblasts, osteocytes and osteoclasts. The bone matrix consists of organic matrix (mostly type I collagen) and inorganic matrix (carbonated hydroxyapatite) [135]. There are many approaches to bone tissue engineering, and the most common strategies are incorporation of calcium phosphate or growth factors into or on a scaffold and seeding and differentiating bone marrow stromal cells (MSCs) or osteoblast-like cells [136]. The engineered bone is often assessed for its compressive strength, toughness, appropriate cell composition and matrix deposition.

For bone tissue engineering application, Jin et al. [137] demonstrated the potential of electrospun silk matrices to support MSC attachment, proliferation and ECM deposition, observing improved cell attachment for PEO-extracted matrices compared to non-extracted matrices. However, no difference was observed in cell proliferation. With mouse osteoblast-like cells (MC3T3-E1), Meechaisue et al. also demonstrated the potential of electrospun silk matrices for bone applications [79].

The MC3T3-E1 cells were also used for bone regeneration studies with silk electrospun matrices. Kim et al. [138] found significantly increased osteocalcin protein content in cell culture medium on day 14 compared to days 1 and 7. When compared with tissue culture plastic, silk nanofibrous matrices showed comparable cellular response in terms of alkaline phosphatase (ALPase) activity and mineralization (calcium phosphate deposition). To study silk matrices capacity for guided bone growth, silk matrices were implanted into 8-mm-diameter full-thickness calvarial defects in adult male New Zealand White rabbits. Results showed significantly improved new bone formation at the defect area with silk grafts compared to sham surgery control groups. Moreover, complete defect closure was observed in grafted animals while only partial bone repair on the periphery of the defect was observed for control groups (Fig. 12). Additionally, in the grafted group osteocyte-like cells appeared inside the new bone and multinucleated cells were absent from the surrounding tissue.

In another study, 3-D silk matrices prepared by a modified electrospinning technique were fabricated and used for bone generation with MC3T3-E1 cells [100]. Significantly improved cell spreading and proliferation were observed on 3-D silk matrices compared to 2-D matrices. Enhanced cell adhesion through integrin-mediated engagement on 3-D scaffolds was confirmed with increased phosphorylation of paxillin Tyr118, FAK Tyr397, and c-Src Tyr416. The higher porosity of 3-D matrices was attributed to the improved cell adhesion and spreading.

Using electrospinning, growth factors can be easily incorporated into fibers to enhance their ability in bone formation. Li et al. successfully

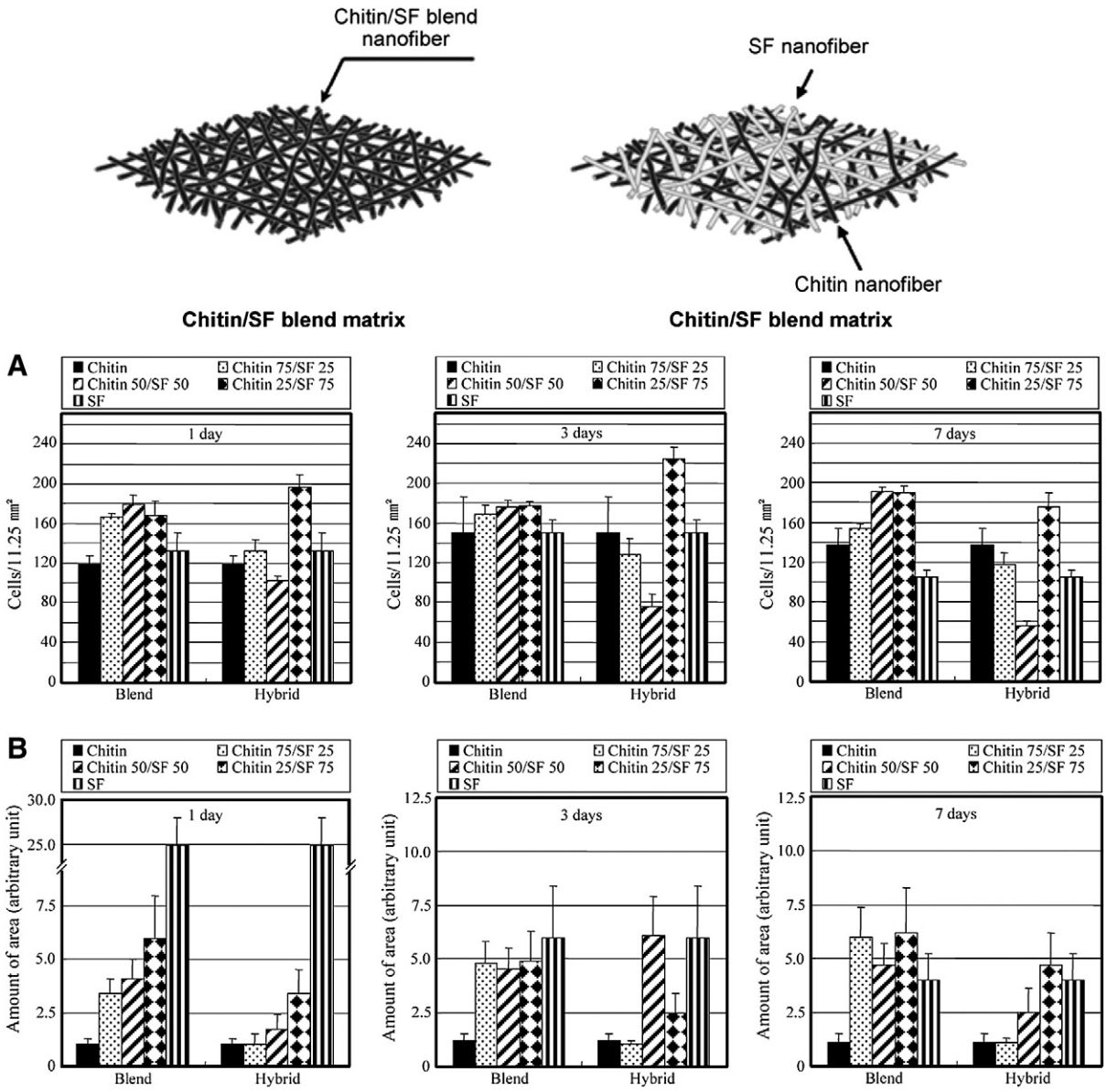

Fig. 11. (A) Schematic structure of chitin/silk fibroin biocomponent nanofibrous scaffolds. (B) Cell attachment (a) and relative spreading area (b) of normal human keratinocytes on chitin/SF blend and hybrid nanofibrous matrices without coating for 0, 1, 3, and 7 days of culture. The relative spreading levels were obtained by normalize the spreading area with that from cells cultured on pure chitin nanofibrous matrix for 1 day. Data are expressed as the mean ± S.E. ($n = 30$). S.E.: standard error of the mean. (From Ref. [134] with permission).

encapsulated BMP-2 and nanoparticles of hydroxyapatite (nHAP) into silk electrospun matrices alone or in combination. These functionalized silk matrices were seeded with hMSCs and assessed for bone formation [104]. BMP-2 incorporated matrices demonstrated increased calcium deposition, apatite crystallinity and transcript levels of bone-specific markers compared to matrices without BMP-2. The highest calcium deposition and BMP-2 transcript level were observed for fibers containing both BMP-2 and nHAP, indicating that these matrices were efficient at delivering BMP-2 and nHAP, and the mild aqueous process preserved the bioactivity of incorporated biomolecules (Fig. 13).

6.4. Cartilage

Cartilage, another type of dense connective tissue, contains chondrocytes sparsely incorporated in non-vascularized, non-innervated ECM. The ECM is composed of abundant ground substance rich in proteoglycans and strengthened by collagen or sometimes elastin fibers depending on cartilage type [139]. Cartilage is found in many areas in the body, including the rib cage, ear, intervertebral discs and articular surfaces between bones. It provides structure and support to the body's tissues without the rigidity of bone, and provides cushioning in joints. Cartilage defects usually result from aging, joint injury and developmental disorders, which often cause joint pain and loss of mobility. In cartilage ECM, cells are supported solely by nutrient and gas through diffusion and this combined with low cell density provides cartilage limited capacity of self-repair [140].

Electrospun silk matrices with microwave-induced argon plasma treatment have been demonstrated as a potential candidate for cartilage repair [141]. Plasma treatment significantly increased attachment and proliferation of neonatal human knee articular chondrocytes. Moreover, glycosaminoglycan (GAG) synthesis was significantly elevated on plasma-treated silk matrices within one day after cell seeding. However, no difference was observed after one week of cell culture, suggesting that plasma treatment is only effective in the early stages of culture.

Electrospun silk matrices have demonstrated potential as tissue engineering scaffolds for vascular graft, skin, bone and cartilage

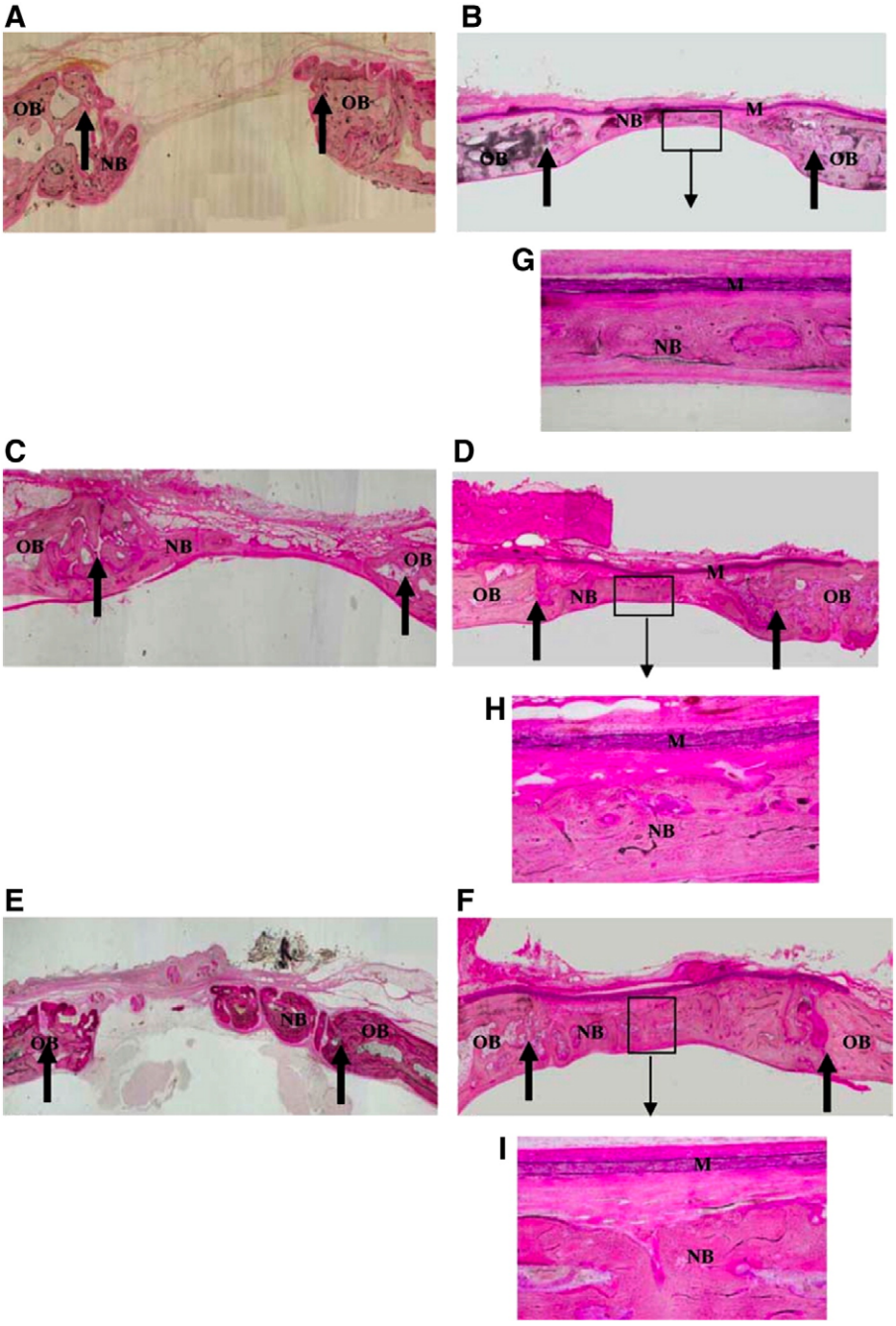

Fig. 12. Histological observation of silk fibroin (SF) nanofiber membrane in rabbit calvarial defects: control group at (A) 4, (C) 8 and (E) 12 weeks (20×); SF nanofiber membrane implanted group at (B,H) 4, (D,I) 8 and (F,G) 12 weeks at (B,D,F) lower (20×) and (H,I,G) higher (100×) magnification. M: the SF nanofiber membrane; NB: new bone; OB: old bone; Arrow: wound edge. The samples were stained with multiple stain solution. (From Ref. [138] with permission).

applications. Applying these matrices for other tissue applications should also be promising due to the unique properties of silk fibroin biomaterial.

7. Future prospects

With the evolution of scaffold design for tissue engineering, electrospinning has attracted interest due to its ability to produce nanofibrous scaffolds mimicking certain fibrous structures of native ECM. Electrospinning is the simplest and most effective method for fabrication of continuous nanofibers. A variety of biodegradable polymers have been successfully electrospun into nano- to micro-fibers, with accelerated research into novel processing and material options in the last two decades. Yet many challenges still exist in the electrospinning process and a number of fundamental questions remain unanswered.

Extensive studies have been performed to elucidate the factors that affect electrospinning and relationships between these factors and the resulting fiber characteristics. However, it is still difficult to predict the outcome from an electrospinning process due to the complex and interrelated effects from various parameters. For example, polymer solution viscosity combines multiple effects from chemical interactions, molecular weight and solution concentration, and is an important factor in determining solution spinnability. Yet this parameter still cannot be used as a universal parameter to predict spinnability between polymers. This suggests the existence of other factors that affect spinnability that are not reflected in viscosity. Hence, a dimensionless parameter or formula used for determining

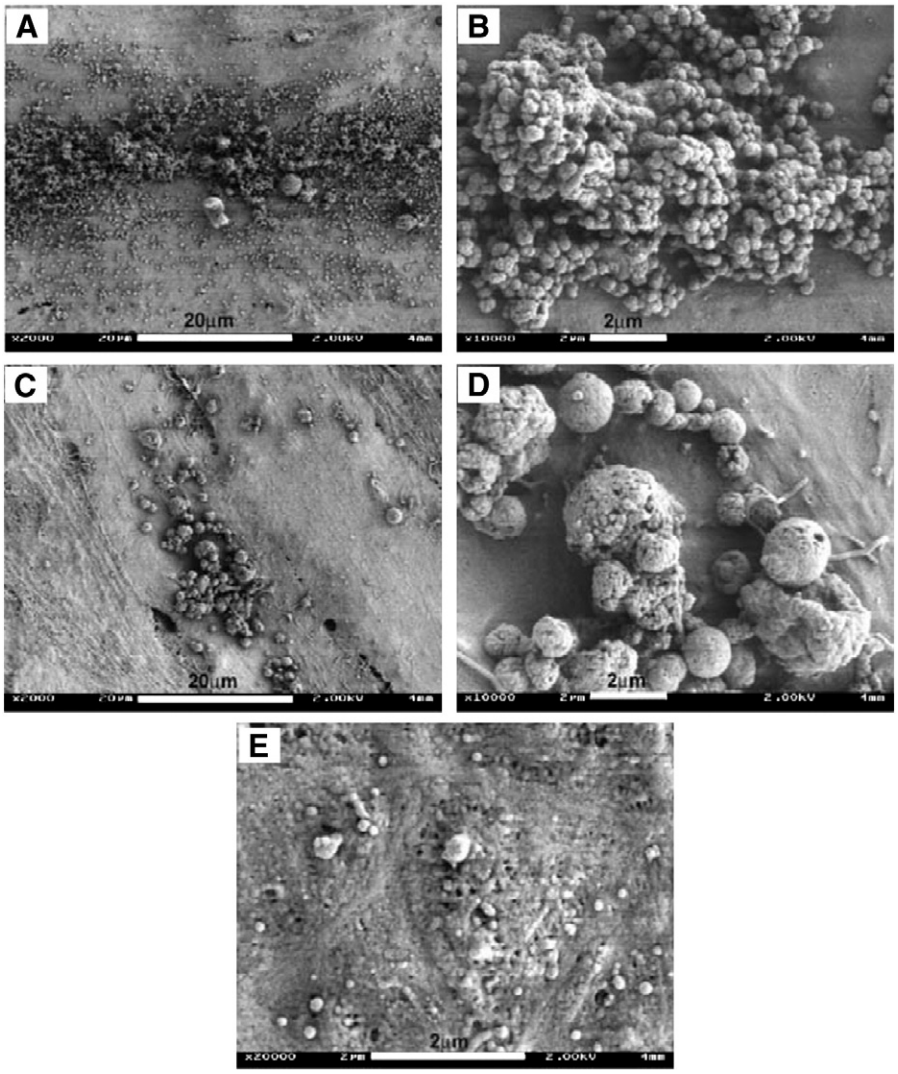

Fig. 13. Comparison between SEM micrographs of hMSCs cultured on silk fibroin electrospun fibrous mats (a,b) without and (c–e) with incorporation of BMP-2 for 31 days. (From Ref. [104] with permission).

the spinnability of polymer solutions in an electrospinning process is still needed.

A second challenge in electrospinning is obtaining nanofibers with uniform diameter and without bead defects. The limited understanding of bead formation and the uncertainty of process control remain an issue. A unique challenge for naturally derived biomaterials (including silk fibroin) is maintaining batch-to-batch consistency due to the variation of material source as well as material processing. So far, most of the electrospun fibers proposed for tissue engineering are obtained from synthetic biomaterials; thus more effort is needed to explore the potential of natural-origin polymers for the reasons stated earlier.

Although many studies have been performed to understand the process of electrospinning, little is known regarding polymer chain conformational changes during the electrospinning process. Solvents and polymer chemical formula are expected to have a crucial role in defining conformational changes. A related systematic study of these parameters would improve predictability and reproducibility of spun fiber products. Additionally, functionalized electrospun fibers have demonstrated to improve cellular responses, but little is known concerning the influence of the electrospinning process on drug loading and release. Further exploration of research on these aspects is necessary to be able to control the process of drug loading and delivery.

Many different electrospun polymeric scaffolds, including silk, have been tested with diverse cell types, but most research thus far is still restricted to preliminary, qualitative analyses of biocompatibility *in vitro*, with only a few studies executed *in vivo*. More *in vivo* studies are needed, as are more quantitative evaluations of cellular function resulting from topographical cues provided by nanofiberous scaffolds. Long-term evaluation of modified or un-modified nanofibrous scaffolds *in vivo* will become critical in the field.

Acknowledgements

This work was supported by the NIH P41 Tissue Engineering Resource Center, the NSF and the AFOSR. The authors would like to gratefully thank Cassandra B Baughma, Evangelia Bellas and Vinny Keshav for their assistance in preparation of this review.

References

[1] R. Skalak, C.F. Fox (Eds.), Tissue Engineering, Alan R Liss, Inc., New York.
[2] J.P. Vacanti, C.A. Vacanti, The challenge of tissue engineering, in: R. Lanza, R. Langer, W. Chick (Eds.), Principles of Tissue Engineering, Academic Press, San Diego, CA, 1997, pp. 1–5.
[3] C.J. Koh, A. Atala, Tissue engineering, stem cells, and cloning: opportunities for regenerative medicine, J. Am. Soc. Nephrol. 15 (2004) 1113–1125.
[4] R. Langer, J.P. Vacanti, Tissue engineering, Science 260 (1993) 920–926.

[5] S.P. Hoerstrup, J.P. Vacanti, Overview of tissue engineering, in: B.D. Ratner, A.S. Hoffman, F.J. Schoen (Eds.), Biomaterial Science: An Introduction to Materials in Medicine, 2nd ed, Elsvier Academic Pr., 2004, pp. 712–727.
[6] R. Murugan, S. Ramakrishna, Nano-featured scaffolds for tissue engineering: a review of spinning methodologies, Tissue Eng. 12 (2006) 435–447.
[7] C.P. Barnes, S.A. Sell, E.D. Boland, D.G. Simpson, G.L. Bowlin, Nanofiber technology: designing the next generation of tissue engineering scaffolds, Adv. Drug Deliv. Rev. 59 (2007) 1413–1433.
[8] S. Kidoaki, I.K. Kwon, T. Matsuda, Mesoscopic spatial designs of nano- and microfiber meshes for tissue-engineering matrix and scaffold based on newly devised multilayering and mixing electrospinning techniques, Biomaterials 26 (2005) 37–46.
[9] R. Murugan, S. Ramakrishna, Design strategies of tissue engineering scaffolds with controlled fiber orientation, Tissue Eng. 13 (2007) 1845–1866.
[10] M.P. Lutolf, J.A. Hubbell, Synthetic biomaterials as instructive extracellular microenvironments for morphogenesis in tissue engineering, Nat Biotechnol. 23 (2005) 47–55.
[11] S. Liao, B. Li, Z. Ma, H. Wei, C. Chan, S. Ramakrishna, Biomimetic electrospun nanofibers for tissue regeneration, Biomed Mater. 1 (2006) R45–53.
[12] K.S. Rho, L. Jeong, G. Lee, B.M. Seo, Y.J. Park, S.D. Hong, S. Roh, J.J. Cho, W.H. Park, B.M. Min, Electrospinning of collagen nanofibers: effects on the behavior of normal human keratinocytes and early-stage wound healing, Biomatrials 27 (2006) 1452–1461.
[13] C.T. Laurencin, A.M. Ambrosio, M.D. Borden, J.A. Cooper Jr., Tissue engineering: orthopedic applications, Annu. Rev. Biomed. Eng. 1 (1999) 19–46.
[14] K. Jayaraman, M. Kotaki, Y. Zhang, X. Mo, S. Ramakrishna, Recent advances in polymer nanofibers, J. Nanosci. Nanotechnol. 4 (2004) 52–65.
[15] Z. Ma, M. Kotaki, R. Inai, S. Ramakrishna, Potential of nanofiber matrix as tissue-engineering scaffolds, Tissue Eng. 11 (2005) 101–109.
[16] X. Wen, D. Shi, N. Zhang, Applications of nanotechnology in tissue engineering, in: H. Nalwa (Ed.), Handbook of Nanostructured Biomaterials and Their Applications in Nanobiotechnology, American Scientific Publishers, Stevenson Ranch, CA, 2005, pp. 1–23.
[17] L.A. Smith, P.X. Ma, Nano-fibrous scaffolds for tissue engineering, Colloids Surf. B Biointerfaces 39 (2004) 125–131.
[18] T.J. Sill, H.A. von Recum, Electrospinning: applications in drug delivery and tissue engineering, Biomaterials 29 (2008) 1989–2006.
[19] N. Minoura, S. Aiba, M. Higuchi, Y. Gotoh, M. Tsukada, Y. Imai, Attachment and growth of fibroblast cells on silk fibroin, Biochem. Biophys. Res. Commun. 208 (1995) 511–516.
[20] J.R. Mauney, T. Nguyen, K. Gillen, C. Kirker-Head, J.M. Gimble, D.L. Kaplan, Engineering adipose-like tissue *in vitro* and *in vivo* utilizing human bone marrow and adipose-derived mesenchymal stem cells with silk fibroin 3D scaffolds, Biomaterials 28 (2007) 5280–5290.
[21] X. Zhang, C.B. Baughman, D.L. Kaplan, *In vitro* evaluation of electrospun silk fibroin scaffolds for vascular cell growth, Biomaterials 29 (2008) 2217–2227.
[22] C. Vendrely, T. Scheibel, Biotechnological production of spider-silk proteins enables new applications, Macromol. Biosci. 7 (2007) 401–409.
[23] Y. Wang, D.D. Rudym, A. Walsh, L. Abrahamsen, H.J. Kim, H.S. Kim, C. Kirker-Head, D.L. Kaplan, *In vivo* degradation of three-dimensional silk fibroin scaffolds, Biomaterials 29 (2008) 3415–3428.
[24] P.M. Cunniff, S.A. Fossey, M.A. Auerbach, J.W. Song, D.L. Kaplan, W.W. Adams, R.K. Eby, D. Mahoney, D.L. Vezie, Mechanical and thermal properties of dragline silk from the spider, *Nephila clavipes*, Polym. Adv. Technol. 5 (1994) 401–410.
[25] J. Magoshi, Y. Magoshi, Physical properties and structure of silk. V. Thermal behavior of silk fibroin in the random-coil conformation, J. Polym. Sci. Japan 15 (1977) 1675–1683.
[26] S. Nakamura, J. Magoshi, Y. Magoshi, Thermal properties of silk proteins in silkworms, in: D.L. Kaplan, W.W. Adams, B. Farmer, C. Viney (Eds.), Silk Polymers: Materials Science and Biotechnology, Ser. 544, ACS Symp, 1994, pp. 211–221.
[27] J. Zeleny, The electrical discharge from liquid points and ahydrostatic method of measuring the electric intensity at their surfaces, J. Phy. Rev. 3 (1914) 69–91.
[28] A. Formhals, U. S. Patent 975 (1934) 504.
[29] A. Formhals, U. S. Patent 160 (1939) 962.
[30] A. Formhals, U. S. Patent 187 (1940) 306.
[31] A. Formhals, U. S. Patent 323 (1943) 025.
[32] A. Formhals, U. S. Patent 349 (1944) 950.
[33] P.K. Baumgarten, Electrostatic spinning of acrylic microfibers, J. Colloid Interface Sci. 36 (1971) 71–79.
[34] H.L. Simons, U.S. Patent 280 (1966) 229.
[35] G.I. Taylor, Electrically driven jets, Proc. R. Soc. London 313A (1969) 453–475.
[36] D. Annis, A. Bornat, R.O. Edwards, A. Higham, B. Loveday, J. Wilson, An elastomeric vascular prosthesis, Trans. Am. Soc. Artif. Intern. Organs 24 (1978) 209–214.
[37] A.C. Fisher, L.D. Cossart, T.V. How, D. Annis, Long term *in-vivo* performance of an electrostatically-spun small bore arterial prosthesis: the contribution of mechanical compliance and anti-platelet therapy, Life Support Syst. 1 (1985) 462–465.
[38] Z.M. Huang, Y.Z. Zhang, M. Kotaki, S. Ramakrishna, A review on polymer nanofibers by electrospinning and their applications in nanocomposites, Compos. Sci. Technol. 63 (2003) 2223–2253.
[39] H.L. Schreuder-Gibson, P. Gibson, Protective textile based on electrospun nanofibers, J. Adv. Mater. 34 (2002) 44–55.
[40] P.P. Tsaia, H. Schreuder-Gibson, P. Gibson, Different electrostatic methods for making electret filters, J. Electrostatic 54 (2002) 333–341.
[41] D.H. Peneker, I. Chun, Nanometer diameter fibers of polymer produced by electrospinning, Nanotechnology 7 (1996) 216–223.
[42] S. Megelski, J.S. Stephens, J.F. Rabolt, C.D. Bruce, Micro- and nanostructured surface morphology on electrospun polymer fibers, Macromolecules 35 (2002) 8456–8466.
[43] L.S. Nair, S. Bhattacharyya, C.T. Laurencin, Development of novel tissue engineering scaffolds via electrospinning, Expert Opin. Biol. Ther. 4 (2004) 659–668.
[44] M.M. Hohman, M. Shin, G. Rutledge, M.P. Brenner, Electrospinning and electrically forced jets I. Stability theory, Phys. Fluids 13 (2001) 2201–2220.
[45] M.M. Hohman, M. Shin, G. Rutledge, M.P. Brenner, Electrospinning and electrically forced jets. II Applications, Phys. Fluids 13 (2001) 2221–2236.
[46] X. Fang, D.H. Reneker, DNA fibers by electrospinning, J. Macromol. Sci., Phys. B36 (1997) 169–173.
[47] H. Fong, D.H. Reneker, Electrospinning and formation of nanofibers, in: D.R. Salem (Ed.), Structure Formation in Polymeric Fibers, Hanser, Munich, 2001, pp. 225–246.
[48] J.M. Deitzel, J. Kleinmeyer, D. Harrus, N.C. Beck Tan, The effect of processing variables on the morphology of electrospun nanofibers and textiles, Polymer 42 (2001) 261–272.
[49] A.L. Yarin, S. Koombhongse, D.H. Reneker, Bending instability in electrospinning nanofibers, J. Appl. Phys. 89 (2001) 3018–3026.
[50] D.H. Reneker, A.L. Yarin, H. Fong, S. Koombhongse, Bending instability of electrically charged liquid jets of polymer solutions in electrospinning, J. appl. Phys. 87 (2000) 4531–4547.
[51] J. Doshi, D.H. Reneker, Electrospinning process and applications of electrospun fibers, J. Electrostat. 35 (1995) 151–160.
[52] S. Warner, A. Buer, M. Grimler, S. Ugbolue, G. Rutledge, M. Shin, Nano fibers, Natl. Text, Cent. Annu. Rep. (1998) 83.
[53] Y.M. Shin, M.M. Hohman, M.P. Brenner, G.C. Rutledge, Electrospinning: a whipping fluid jet generates submicron polymer fibers, Appl. Phys. Lett. 78 (2001) 1149–1151.
[54] S. Ramakrishna, K. Fujihara, W.E. Teo, T. Yong, Z. Ma, R. Ramaseshaa, Electrospun nanofibers: solving global issues, Materials Today 9 (2006) 40–50.
[55] I. Hayati, A.I. Bailey, T.F. Tadros, Investigation into the mechanism of electro-hydrodynamic spraying of liquids, I. Effect of electric field the environment on pendant drops and factors affecting the formation of stable jets and atomization, J. Colloid Interf. Sci. 117 (1987) 205–221.
[56] J.M. Dietzel, J. Kleinmeyer, D. Harris, N.C. Beck Tan, The effect of processing variables on the morphology of electrospun nanofibers and textiles, Polymer 42 (2001) 261–272.
[57] T. Subbiah, G.S. Bhat, R.W. Tock, S. Parameswaran, S.S. Ramkumar, Electrospinning of nanofibers, J. Appl. Polym. Sci. 96 (2005) 557–569.
[58] J. Kameoka, R. Orth, Y. Yang, D. Czaplewski, R. Mathers, G.W. Coates, H.G. Craighead, A scanning tip electrospinning source for deposition of oriented nanofibres, Nanotechnology 14 (2003) 1124–1129.
[59] X.H. Zong, K. Kim, D.F. Fang, S.F. Ran, B.S. Hsiao, B. Chu, Structure and process relationship of electrospun bioabsorbable nanofiber membranes, Polymer 43 (2002) 4403–4412.
[60] H.S. Kim, K. Kim, H.J. Jin, I.J. Chin, Morphological characterization of electrospun nano-fibrous membranes of biodegradable poly(L-lactide) and poly(lactideco-glycolide), Macromol. Symp. 224 (2005) 145–154.
[61] J.M. Deitzel, J. Kleinmeyer, D. Harris, N.C.B. Tan, The effect of processing variables on the morphology of electrospun nanofibers and textiles, Polymer 42 (2001) 261–272.
[62] W.K. Son, J.H. Youk, T.S. Lee, W.H. Park, The effects of solution properties and polyelectrolyte on electrospinning of ultrafine poly(ethylene oxide) fibers, Polymer 45 (2004) 2959–2966.
[63] C.X. Zhang, X.Y. Yuan, L.L. Wu, Y. Han, J. Sheng, Study on morphology of electrospun poly(vinyl alcohol) mats, Eur. Polym. J. 41 (2005) 423–432.
[64] P. Gupta, C. Elkins, T.E. Long, G.L. Wilkes, Electrospinning of linear homopolymers of poly(methyl methacrylate): exploring relationships between fiber formation, viscosity, molecular weight and concentration in a good solvent, Polymer 46 (2005) 4799–4810.
[65] T. Jarusuwannapoom, W. Hongroijanawiwat, S. Jitjaicham, L. Wannatong, M. Nithitanakul, C. Pattamaprom, P. Koombhongse, R. Rangkupan, P. Supaphol, Effect of solvents on electro-spinnability of polystyrene solutions and morphological appearance of resulting electrospun polystyrene fibers, Eur. Polym. J. 41 (2005) 409–421.
[66] A. Koski, K. Yim, S. Shivkumar, Effect of molecular weight on fibrous PVA produced by electrospinning, Mater. Lett. 58 (2004) 493–497.
[67] J.S. Lee, K.H. Choi, H. Do Ghim, S.S. Kim, D.H. Chun, H.Y. Kim, W.S. Lyoo, Role of molecular weight of atactic poly(vinyl alcohol) (PVA) in the structure and properties of PVA nanofabric prepared by electrospinning, J. Appl. Polym. Sci. 93 (2004) 1638–1646.
[68] K. Ohgo, C. Zhao, M. Kobayashi, T. Asakura, Preparation of non-woven nanofibers of *Bombyx mori* silk, *Samia Cynthia ricini* silk and recombinant hybrid silk with electrospinning method, Polymer 44 (2003) 841–846.
[69] L. Jeong, K.Y. Lee, W.H. Park, Effect of solvent on the characteristics of electrospun regenerated silk fibroin nanofibers, Key Eng. Mater. 342–343 (2007) 813–816.
[70] H. Wang, H. Shao, X. Hu, Structure of silk fibroin fibers made by an electrospun process from a silk fibroin aqueous solution, J. Appl. Polym. Sci. 101 (2006) 961–968.
[71] H. Wang, Y. Zhang, H. Shao, X. Hu, Electrospun ultra-fine silk fibroin fiber from aqueous solutions, J. Mater. Sci. 40 (2005) 5359–5363.
[72] H.J. Jin, S.V. Fridrikh, G.C. Rutledge, D.L. Kaplan, Electrospinning *Bombyx mori* silk with poly(ethylene oxide), Biomacromolecules 3 (2002) 1233–1239.
[73] J. Zhu, H. Shao, X. Hu, Morphology and structure of electrospun mats from regenerated silk fibroin aqueous solutions with adjusting pH, Int. J. Biol. Macromol. 41 (2007) 469–474.

[74] J. Zhu, Y. Zhang, H. Shao, X. Hu, Electorspinning and rheology of regenerated *Bombyx mori* silk fibroin aqueous solutions: the effects of pH and concentration, Polymer 49 (2008) 2880–2885.
[75] D.S. Katti, K.W. Robinson, F.K. Ko, C.T. Laurencin, Bioresorbable nanofiber-based systems for wound healing and drug delivery: optimization of fabrication parameters, J. Biomed. Mater. Res. 70b (2004) 286–296.
[76] J. Magoshi, Y. Magoshi, M.A. Becker, S. Nakamura, in: J.C. Salamone (Ed.), Polymeric Materials Encyclopedia, CRC Press Inc, Boca Raton, FL, 1996, pp. 667–679.
[77] C. Lu, P. Chen, J. Li, Y. Zhang, Computer simulation of electrospinning. Part I. Effect of solvent in electrospinning, Polymer 47 (2006) 915–921.
[78] S. Sukigara, M. Gandhi, J. Ayutsede, M. Micklus, F. Ko, Regeneration of *Bombyx mori* silk by electrospinning—part 1: processing parameters and geometric properties, Polymer 44 (2003) 5721–5727.
[79] C. Meechaisue, P. Wutticharoenmongko, R. Waraput, T. Huangjing, N. Ketbumrung, P. Pavasant, P. Supaphol, Preparation of electrospun silk fibroin fiber mats as bone scaffolds: a preliminary study, Biomed. Mater. 2 (2007) 181–188.
[80] J.S. Choi, S.W. Lee, L. Jeong, S.H. Bae, B.C. Min, J.H. Youk, W.H. Park, Effect of organosoluble salts on the nanofibrous structure of electrospun poly(3-hydroxybutyrate-co-3-hydroxyvalerate), Int. J. Biol. Macromol. 34 (2004) 249–256.
[81] D.H. Reneker, I. Chun, Nanometre diameter fibres of polymer, produced by electrospinning, Nanotechnology 7 (1996) 216–223.
[82] C.S. Ki, D.H. Baek, K.D. Gang, K.H. Lee, I.C. Um, Y.H. Park, Characterization of gelatin nanofiber prepared from gelatin–formic acid solution, Polymer 46 (2005) 5094–5102.
[83] J.S. Lee, K.H. Choi, H. Do Ghim, S.S. Kim, D.H. Chun, H.Y. Kim, W.S. Lyoo, Role of molecular weight of atactic poly(vinyl alcohol) (PVA) in the structure and properties of PVA nanofabric prepared by electrospinning, J. Appl. Polym. Sci. 93 (2004) 1638–1646.
[84] S. Sukigara, M. Gandhi, J. Ayutsede, M. Micklus, F. Ko, Regeneration of *Bombyx mori* silk by electrospinning. Part 2. Process optimization and empirical modeling using response surface methodology, Polymer 45 (2004) 3701–3708.
[85] J. Ayutsede, M. Gandhi, S. Sukigara, M. Micklus, H.E. Chen, F. Ko, Regeneration of *Bombyx mori* silk by electrospinning. Part 3: characterization of electrospun nonwoven mat, Polymer 46 (2005) 1625–1634.
[86] X.N. Peng, X. Chen, P.Y. Wu, Z.Z. Shao, Investigation on the conformation transition of regenerated silk fibroin films under thermal treatment by two-dimensional (2D) correlation FT-IR spectroscopy, Acta Chim. Sin. 62 (2004) 2127–2130.
[87] D. Wilson, R. Valluzzi, D.L. Kaplan, Conformational transitions in model silk peptides, Biophys. J. 78 (2000) 2690–2701.
[88] M. Ishida, T. Asakura, M. Yokoi, H. Saito, Solvent- and mechanical-treatment-induced conformational transition of silk fibroins studies by high-resolution solid-state carbon-13 NMR spectroscopy, Macromolecules 23 (1990) 88–94.
[89] M. Tsukada, Y. Gotoh, M. Nagura, N. Minoura, N. Kasai, G. Freddi, Structural changes of silk fibroin membranes induced by immersion in methanol aqueous solutions, J. Polym. Sci., Part B: Polym. Phys. 32 (1994) 961–968.
[90] S.H. Kim, Y.S. Nam, T.S. Lee, W.H. Park, Silk fibroin nanofiber. Electrospinning, properties, and structure, Polym. J. 35 (2003) 185–190.
[91] H.J. Jin, J. Park, V. Karageorgiou, U.J. Kim, R. Valluzzi, P. Cebe, D.L. Kaplan, Water-stable silk films with reduced-sheet content, Adv. Funct. Mater. 15 (2005) 1241–1247.
[92] T. Asakura, M. Demura, Y. Watanabe, K. Sato, ^{1}H pulsed NMR study of *Bombyx mori* silk fibroin: dynamics of fibroin and of absorbed water, J. Polym. Sci., Part B: Polym. Phys. 30 (1992) 693–699.
[93] B.M. Min, L. Jeong, K.Y. Lee, W.H. Park, Regenerated silk fibroin nanofibers: water vapor-induced structural changes and their effects on the behavior of normal human cells, Macromol. Biosci. 6 (2006) 285–292.
[94] L. Jeong, K.Y. Lee, J.W. Liu, W.H. Park, Time-resolved structural investigation of regenerated silk fibroin nanofibers treated with solvent vapor, Int. J. Biol. Macromol. 38 (2006) 140–144.
[95] P. Gupta, G.L. Wilkes, Some investigations on the fiber formation by utilizing a side-by-side bicomponent electrospinning approach, Polymer 44 (2003) 6353–6359.
[96] W.H. Park, L. Jeong, D.I. Yoo, S. Hudson, Biomimetic nanofibrous scaffolds: preparation and characterization of chitin/silk fibroin blend nanofibers, Polymer 45 (2004) 7151–7157.
[97] C.R. Yoo, I.S. Yeo, K.E. Park, J.H. Park, S.J. Lee, W.H. Park, B.M. Min, Effect of chitin/silk fibroin nanofibrous bicomponent structures on interaction with human epidermal keratinocytes, Int. J. Biol. Macromol. 42 (2008) 324–334.
[98] I.S. Yeo, J.E. Oh, L. Jeong, T.S. Lee, S.J. Lee, W.H. Park, B.M. Min, Collagen-based biomimetic nanofibrous scaffolds: preparation and characterization of collagen/silk fibroin bicomponent nanofibrous structures, Biomacromolecules 9 (2008) 1106–1116.
[99] M. Wang, J.H. Yu, D.L. Kaplan, G.C. Rutledge, Production of submicron diameter silk fibers under benign processing conditions by two-fluid electrospinning, Macromolecules 39 (2006) 1102–1107.
[100] C.S. Ki, S.Y. Park, H.J. Kim, H.M. Jung, K.M. Woo, J.W. Lee, Y.H. Park, Development of 3-D nanofibrous fibroin scaffold with high porosity by electrospinning: implications for bone regeneration, Biotechnol. Lett. 30 (2008) 405–410.
[101] Y.Z. Zhang, J. Venugopal, Z.M. Huang, C.T. Lim, S. Ramakrishna, Characterization of the surface biocompatibility of the electrospun PCL-collagen nanofibers using fibroblast, Biomacromolecules 6 (2005) 2583–2589.
[102] J. Venugopa, S. Low, A.T. Choon, S. Ramakrishna, Interaction of cell and nanofiber scaffolds in tissue engineering, J. Biomed. Mater. Res. 84B (2007) 34–48.
[103] K.H. Lee, C.S. Ki, E.H. Baek, G.D. Kang, D.W. Ihm, Y.H. Park, Application of electrospun silk fibroin nanofibers as an immobilization support of enzyme, Fibers Polym. 6 (2005) 181–185.
[104] C. Li, C. Vepari, H.J. Jin, H.J. Kim, D.L. Keplan, Electrospun silk-BMP-2 scaffolds for bone tissue engineering, Biomaterials 27 (2006) 3115–3124.
[105] M. Kang, S. Jung, H.S. Kim, J.H. Youk, H.J. Jin, Silver nanoparticles incorporated electrospun silk fibers, J. Nanosci. Nanotechnol. 7 (2007) 3888–3891.
[106] M. Kang, H.J. Jin, Electrically conducting electrospun silk membranes fabricated by adsorption of carbon nanotubes, Colloid. Polym. Sci. 285 (2007) 1163–1167.
[107] S.H. Saw, K. Wang, T. Yong, S. Ramakrishna, Polymeric Nanofibers for Tissue Engineering, in: C.S.S.R. Kumar (Ed.), Nanotechnologies for the Life Sciences, vol. 9, Wiley-VCH, Weinheim, Germany, 2007, pp. 66–134.
[108] W. Li, C.T. Laurencin, E.J. Caterson, R.S. Tuan, F.K. Ko, Electrospun nanofibrous structure: a novel scaffold for tissue engineering, J. Biomed. Mater. Res. 60 (2002) 613–621.
[109] S.R. Bhattarai, N. Bhattarai, H.K. Yi, P.H. Hwang, D. Cha, H.Y. Kim, Novel biodegradable electrospun membrane: scaffold for tissue engineering, Biomaterials 25 (2002) 2595–2602.
[110] C.Y. Xu, R. Inai, M. Kotaki, S. Ramakrishna, Aligned biodegradable nanofibrous structure: a potential scaffold for blood vessel engineering, Biomaterials 25 (2004) 877–886.
[111] Y. Zhang, H. Ouyang, C.T. Lim, S. Ramakrishna, Z. Huang, Electrospinning of gelatin fibers and gelatin/PCL composite fibrous scaffolds, J. Biomed. Mater. Res. Part B: App. Biomaterials 72 (2005) 156–165.
[112] E.D. Boland, J.A. Matthews, K.J. Pawlowski, D.G. Simpson, G.E. Wnek, G.L. Bowlin, Electrospinning collagen and elastin: preliminary vascular tissue engineering, Front. Biosci. 9 (2004) 1422–1432.
[113] J.A. Matthews, E.D. Boland, G.E. Wnek, D.G. Simpson, G.L. Bowlin, Electrospinning of collagen type II: a feasibility study, J. Bioact. Compat. Polym. 18 (2003) 125–134.
[114] L. Huang, K. Nagapudi, R.P. Apkarian, E.L. Chaikof, Engineered collagen-PEO nanofibers and fabrics, J. Biomater. Sci., Polym. Ed. 12 (2001) 979–993.
[115] I.V. Yannas, J.F. Burke, P.L. Gordon, C. Huang, R.H. Rubenstein, Design of an artificial skin. II. Control of chemical composition, J. Biomed. Mater. Res. 14 (1980) 107–132.
[116] R.R. Brau, I.V. Yannas, Tissue engineering skin, in: G.E. Wnek, G.L. Bowlin (Eds.), Encyclopedia of Biomaterials and Biomedical Engineering, Marcel Dekker, Inc., New York, N.Y., 2004, pp. 1652–1660.
[117] L. Almany, D. Seliktar, Biosynthetic hydrogel scaffolds made from fibrinogen and polyethylene glycol for 3D cell cultures, Biomaterials 26 (2005) 2467–2477.
[118] G.H. Altman, R.L. Horan, H.H. Lu, J. Moreau, I. Martin, J.C. Richmond, D.L. Kaplan, Silk matrix for tissue engineered anterior cruciate ligaments, Biomaterials 23 (2002) 4131–4141.
[119] R.L. Horan, K. Antle, A.L. Collette, Y. Wang, J. Huang, J.E. Moreau, V. Volloch, D.L. Kaplan, G.H. Altman, *In vitro* degradation of silk fibroin, Biomaterials 26 (2005) 3385–3393.
[120] G. Steinthorsson, B. Sumpio, Clinical and biological relevance of vein cuff anastomosis, Acta Chir. Belg. 99 (1999) 282–288.
[121] T. Yokoyama, M.A. Gharavi, Y.C. Lee, W.A. Edmiston, J.H. Kay, Aorta–coronary artery revascularization with an expanded polytetrafluoroethylene vascular graft. A preliminary report, J. Thorac. Cardiovasc. Surg. 76 (1978) 552–555.
[122] R.N. Sapsford, G.D. Oakley, S. Talbot, Early and late patency of expanded polytetrafluoroethylene vascular grafts in aorta–coronary bypass, J. Thorac. Cardiovasc. Surg. 81 (1981) 860–864.
[123] F.J. Veith, S.K. Gupta, E. Ascer, S. White-Flores, R.H. Samson, L.A. Scher, J.B. Towne, V.M. Bernhard, P. Bonier, W.R. Flinn, P. Astelford, J.S.T. Yao, J.J. Bergan, Six year prospective multicenter randomized comparison of autologous saphenous vein and expanded polytetrafluoroethylene grafts in infrainguinal arterial reconstructions, J. Vasc. Surg. 3 (1986) 104–114.
[124] B. Bondara, S. Fuchsa, A. Mottab, C. Migliaresib, C.J. Kirkpatricka, Functionality of endothelial cells on silk fibroin nets: comparative study of micro- and nanometric fibre size, Biomaterials 29 (2008) 561–572.
[125] L. Soffer, X. Wang, X. Zhang, J. Kluge, L. Dorfmann, D.L. Kaplan, G. Leisk, Silk-based electrospun tubular scaffolds for tissue-engineered vascular grafts, J. Biomater. Sci. Polymer Edn. 19 (2008) 653–664.
[126] J.M. Orban, L.B. Wilson, J.A. Kofroth, M.S. El-Kurdi, T.M. Maul, D.A. Vorp, Crosslinking of collagen gels by transglutaminase, J. Biomed. Mater. Res. A 68 (2004) 756–762.
[127] T. Nishibe, Y. Kondo, A. Muto, A. Dardik, Optimal prosthetic graft design for small diameter vascular grafts, Vascular. 15 (2007) 356–360.
[128] M. Rouabhia, Skin substitute production by tissue engineering, Landes Bioscience (1997).
[129] B.M. Min, G. Lee, S.H. Kim, Y.S. Nam, T.S. Lee, W.H. Park, Electrospinning of silk fibroin nanofibers and its effect on the adhesion and spreading of normal human keratinocytes and fibroblasts *in vitro*, Biomaterials 25 (2004) 1289–1297.
[130] B.M. Min, L. Jeong, Y.S. Nam, J.M. Kim, J.Y. Kim, W.H. Park, Formation of silk fibroin matrices with different texture and its cellular response to normal human keratinocytes, Int. J. Biol. Macromol. 34 (2004) 281–288.
[131] B.M. Min, L. Jeong, K.Y. Lee, W.H. Park, Regenerated silk fibroin nanofibers: water vapor-induced structural changes and their effects on the behavior of normal human cells, Macromol. Biosci. 6 (2006) 285–292.
[132] Y. Okamoto, M. Watanabe, K. Miyatake, M. Morimoto, Y. Shigemasa, S. Minami, Effects of chitin/chitosan and their oligomers/monomers on migrations of fibroblasts and vascular endothelium, Biomaterials 23 (2002) 1975–1979.
[133] K.E. Park, S.Y. Jung, S.J. Lee, B.M. Min, W.H. Park, Biomimetic nanofibrous scaffolds: preparation and characterization of chitin/silk fibroin blend nanofibers, Int. J. Biol. Macromol. 38 (2006) 165–173.
[134] C.R. Yoo, I.S. Yeo, K.E. Park, J.H. Park, S.J. Lee, W.H. Park, B.M. Min, Effect of chitin/silk fibroin nanofibrous bicomponent structures on interaction with human epidermal keratinocytes, Int. J. Biol. Macromol. 42 (2008) 324–334.

[135] L.G. Griffith, G. Naughton, Tissue engineering—current challenges and expanding opportunities, Science 295 (2002) 1009–1014.
[136] S. Liao, B. Li, Z. Ma, H. Wei, C. Chan, S. Ramakrishna, Biomimetic electrospun nanofibers for tissue regeneration, Biomed. Mater. 1 (2006) R45–R53.
[137] H.J. Jin, J. Chen, V. Karageorgiou, G.H. Altman, D.L. Kaplan, Human bone marrow stromal cell responses on electrospun silk fibroin mats, Biomaterials 25 (2004) 1039–1047.
[138] K.H. Kim, L. Jeong, H.N. Park, S.Y. Shin, W.H. Park, S.C. Lee, T.I. Kim, Y.J. Park, Y.J. Seol, Y.M. Lee, Y. Ku, I.C. Rhyu, S.B. Han, C.P. Chung, Biological efficacy of silk fibroin nanofiber membranes for guided bone regeneration, J. Biotechnol. 120 (2005) 327–339.
[139] N.P. Morris, D.R. Keene, W.A. Horton, Cartilage, in: P.M. Royce, B. Steinmann (Eds.), Connective Tissue and Its Heritable Disorders: Molecular, Genetic, and Medical Aspects, Wiley-IEEE, 2003, pp. 41–66.
[140] W.J. Li, R. Tuli, C. Okafor, A. Derfoul, K.G. Danielson, D.J. Hall, R.S. Tuan, A three-dimensional nanofibrous scaffold for cartilage tissue engineering using human mesenchymal stem cells, Biomaterials 26 (2005) 599–609.
[141] H.S. Baek, Y.H. Park, C.S. Ki, J.C. Park, D.K. Rahd, Enhanced chondrogenic responses of articular chondrocytes onto porous silk fibroin scaffolds treated with microwave-induced argon plasma, Surf. Coat. Technol. 202 (2008) 5794–5797.
[142] F. Yang, R. Murugan, S. Wang, S. Ramakrishna, Electrospinning of nano/micro scale poly(L-lactic acid) aligned fibers and their potential in neural tissue engineering, Biomaterials 26 (2005) 2603–2610.
[143] S.J. Eichhorn, W.W. Sampson, Statistical geometry of pores and statistics of porous nanofibrous assemblies, J R. Soc. Interface 22 (2005) 309–318.
[144] J. Stitzel, J. Liu, S.J. Lee, M. Komura, J. Berry, S. Soker, G. Lim, M.V. Dyke, R. Czerw, J.J. Yoo, A. Atalac, Controlled fabrication of a biological vascular substitute, Biomaterials 27 (2006) 1088–1094.
[145] Z. Ma, W. He, T. Yong, S. Ramakrishna, Grafting of gelatin on electrospun poly (caprolactone) nanofibers to improve endothelial cell spreading and proliferation and to control cell orientation, Tissue Eng. 11 (2005) 1149–1158.
[146] E. Schnell, K. Klinkhammer, S. Balzer, G. Brook, D. Klee, P. Dalton, J. Mey, Guidance of glial cell migration and axonal growth on electrospun nanofibers of poly-epsilon-caprolactone and a collagen/poly-epsilon-caprolactone blend, Biomaterials 28 (2007) 3012–3025.
[147] H. Inoguchi, T. Tanaka, Y. Maehara, T. Matsuda, The effect of gradually graded shear stress on the morphological integrity of a huvec-seeded compliant small-diameter vascular graft, Biomaterials 28 (2007) 486–495.
[148] S. Zhong, W.E. Teo, X. Zhu, R.W. Beuerman, S. Ramakrishna, L.Y. Yung, An aligned nanofibrous collagen scaffold by electrospinning and its effects on *in vitro* fibroblast culture, J. Biomed. Mater. Res. 79A (2006) 456–463.
[149] J.H. Song, H.E. Kim, H.W. Kim, Production of electrospun gelatin nanofiber by water-based co-solvent approach, J. Mater. Sci.: Mater. Med. 19 (2007) 95–102.
[150] I.C. Um, D. Fang, B.S. Hsiao, A. Okamoto, B. Chu, Electro-spinning and electro-blowing of hyaluronic acid, Biomacromolecules 5 (2004) 1428–1436.
[151] C. Ayres, G.L. Bowlin, S.C. Henderson, L. Taylor, J. Shultz, J. Alexander, T.A. Telemeco, D.G. Simpson, Modulation of anisotropy in electrospun tissue-engineering scaffolds: analysis of fiber alignment by the fast Fourier transform, Biomaterials 27 (2006) 5524–5534.
[152] M.C. McManus, E.D. Boland, D.G. Simpson, C.P. Barnes, G.L. Bowlin, Electrospun fibrinogen: feasibility as a tissue engineering scaffold in a rat cell culture model, J. Biomed. Mater. Res. 81A (2007) 299–309.
[153] S. Zarkoob, R.K. Eby, D.H. Reneker, S.D. Hudson, D. Ertley, W.W. Adams, Structure and morphology of electrospun silk nanofibers, Polymer 45 (2004) 3973–3977.
[154] C. Wong Po Foo, S.V. Patwardhan, D.J. Belton, B. Kitchel, D. Anastasiades, J. Huang, R.R. Naik, C.C. Perry, D.L. Kaplan, Novel nanocomposites from spider silk–silica fusion (chimeric) proteins, Proc. Natl. Acad. Sci. U.S.A. 103 (2006) 9428–9433.
[155] S.S. Silva, D. Maniglio, A. Motta, J.F. Mano, R.L. Reis, C. Migliaresi, Genipin-modified silk-fibroin nanometric nets, Macromol. Biosci. 8 (2008) 766–774.
[156] S. Zhou, H. Peng, X. Yu, X. Zheng, W. Cui, Z. Zhang, X. Li, J. Wang, J. Weng, W. Jia, F. Li, Preparation and characterization of a novel electrospun spider silk fibroin/poly(D,L-lactide) composite fiber, J. Phys. Chem. B 36 (2008) 11209–11216.